

**COMPARISON OF DIFFERENT POWER SYSTEM
RESILIENCE ASSESSMENT METHODS**

SAM CHAN JIAN HOW

**FACULTY OF ENGINEERING
UNIVERSITY OF MALAYA
KUALA LUMPUR**

2020

**COMPARISON OF DIFFERENT POWER SYSTEM
RESILIENCE ASSESSMENT METHODS**

SAM CHAN JIAN HOW

**RESEARCH REPORT SUBMITTED IN PARTIAL
FULFILMENT OF THE REQUIREMENTS FOR THE
DEGREE OF MASTER OF POWER SYSTEM
ENGINEERING**

**FACULTY OF ENGINEERING
UNIVERSITY OF MALAYA
KUALA LUMPUR**

2020

UNIVERSITY OF MALAYA
ORIGINAL LITERARY WORK DECLARATION

Name of Candidate: Sam Chan Jian How

Matric No: KQI160014

Name of Degree: Master of Power System Engineering

Comparison of Different Power System Resilience Assessment Methods (“this Work”):

Field of Study:

I do solemnly and sincerely declare that:

- (1) I am the sole author/writer of this Work;
- (2) This Work is original;
- (3) Any use of any work in which copyright exists was done by way of fair dealing and for permitted purposes and any excerpt or extract from, or reference to or reproduction of any copyright work has been disclosed expressly and sufficiently and the title of the Work and its authorship have been acknowledged in this Work;
- (4) I do not have any actual knowledge nor do I ought reasonably to know that the making of this work constitutes an infringement of any copyright work;
- (5) I hereby assign all and every rights in the copyright to this Work to the University of Malaya (“UM”), who henceforth shall be owner of the copyright in this Work and that any reproduction or use in any form or by any means whatsoever is prohibited without the written consent of UM having been first had and obtained;
- (6) I am fully aware that if in the course of making this Work I have infringed any copyright whether intentionally or otherwise, I may be subject to legal action or any other action as may be determined by UM.

Candidate’s Signature

Date:

Subscribed and solemnly declared before,

Witness’s Signature

Date:

Name:

Designation:

UNIVERSITI MALAYA
PERAKUAN KEASLIAN PENULISAN

Nama: Sam Chan Jian How

No. Matrik: KQI160014

Nama Ijazah:

Perbandingan Kaedah Penilaian Daya Tahan Dalam Sistem Kuaza Berbeza
("Hasil Kerja ini"):

Bidang Penyelidikan:

Saya dengan sesungguhnya dan sebenarnya mengaku bahawa:

- (1) Saya adalah satu-satunya pengarang/penulis Hasil Kerja ini;
- (2) Hasil Kerja ini adalah asli;
- (3) Apa-apa penggunaan mana-mana hasil kerja yang mengandungi hakcipta telah dilakukan secara urusan yang wajar dan bagi maksud yang dibenarkan dan apa-apa petikan, ekstrak, rujukan atau pengeluaran semula daripada atau kepada mana-mana hasil kerja yang mengandungi hakcipta telah dinyatakan dengan sejelasnya dan secukupnya dan satu pengiktirafan tajuk hasil kerja tersebut dan pengarang/penulisnya telah dilakukan di dalam Hasil Kerja ini;
- (4) Saya tidak mempunyai apa-apa pengetahuan sebenar atau patut semunasabahnya tahu bahawa penghasilan Hasil Kerja ini melanggar suatu hakcipta hasil kerja yang lain;
- (5) Saya dengan ini menyerahkan kesemua dan tiap-tiap hak yang terkandung di dalam hakcipta Hasil Kerja ini kepada Universiti Malaya ("UM") yang seterusnya mula dari sekarang adalah tuan punya kepada hakcipta di dalam Hasil Kerja ini dan apa-apa pengeluaran semula atau penggunaan dalam apa jua bentuk atau dengan apa juga cara sekalipun adalah dilarang tanpa terlebih dahulu mendapat kebenaran bertulis dari UM;
- (6) Saya sedar sepenuhnya sekiranya dalam masa penghasilan Hasil Kerja ini saya telah melanggar suatu hakcipta hasil kerja yang lain sama ada dengan niat atau sebaliknya, saya boleh dikenakan tindakan undang-undang atau apa-apa tindakan lain sebagaimana yang diputuskan oleh UM.

Tandatangan Calon

Tarikh:

Diperbuat dan sesungguhnya diakui di hadapan,

Tandatangan Saksi

Tarikh:

Nama:

Jawatan:

ABSTRACT

Climate change has been given significant attention in recent times, calling for more ideas to address issues stemming from extreme weather events. Until climate change can be slowed down and ultimately be reversed, it is an imminent objective to find solutions for the mitigation and prevention of the effects of catastrophic weather events. History has a record of the devastation caused by such events on electrical power infrastructures. While electrical power systems have conventionally been designed and built to weather everyday conditions, confronting cataclysmic high-impact, low-probability events will require more resilient attributes. Power systems are often deemed as the backbone of the operational society, and therefore, the case calling for power infrastructures to be able to withstand critical events is a case carrying compelling weight. The concept of resilience in power systems however, has only emerged in recent times. This study therefore, aims to provide further insights into the area of power system resilience, by focusing on the aftermath of an extreme weather event and how its effects on a power system can be utilized to measure the resilience of the latter. To replicate the random behaviour of weather, windspeeds categorized based on Saffir-Simpson's hurricane scale, were randomly generated following the concept of Monte-Carlo's simulation technique, which would then be applied to fragility curves of distribution poles based on NESC's distribution pole classes. The resilience of the infrastructure is then modelled and assessed by applying the 3 different resilience assessment methods. Finally, evaluations are made to compare the merits and disadvantages of each resilience assessment method.

Keywords: Power System Resilience, Fragility Curve, Resilience Triangle, Resilience Trapezoid, Code-Based Metric.

ABSTRAK

Perubahan iklim telah dijadikan tumpuan perhatian baru-baru ini, dan idea-idea untuk menangani isu-isu yang berpunca daripada kejadian cuaca yang melampau yang secukupnya harus dibincangkan serta diberi perhatian. Sehingga perubahan iklim boleh diperlahankan dan akhirnya dibalikkan, mencari solusi untuk mitigasi dan pencegahan kesan kejadian cuaca bencana adalah wajib. Sejarah mempunyai rekod kemusnahan yang disebabkan oleh kejadian-kejadian akibat cuaca bencana, ke atas infrastruktur kuasa elektrik. Walaupun sistem kuasa elektrik secara konvensional telah direka dan dibina untuk menghadapi keadaan cuaca biasa, akan tetapi, kejadian yang berimpak tinggi walaupun dengan kebarangkalian rendah, memerlukan sifat yang berdaya tahan yang lebih tinggi. Sistem kuasa sering dianggap sebagai tulang belakang masyarakat, dan oleh itu, topik yang melibatkan sifat-sifat system kuasa elektrik untuk menghadapi kes kritikal, harus diberi lebih perhatian dan perbincangan. Konsep ketahanan dalam sistem kuasa bagaimanapun, setakat ini cuma muncul kebelakangan ini. Oleh itu, kajian ini bertujuan untuk memberi pandangan lebih lanjut mengenai bidang daya tahan sistem kuasa, dengan memberi tumpuan kepada peristiwa cuaca ekstrem dan bagaimana kesannya terhadap sistem kuasa dapat digunakan untuk mengukur daya tahan sistem. Untuk meniru perilaku serta ciri-ciri cuaca yang bersifat rawak, kelajuan angin yang dikategorikan berdasarkan skala taufan Saffir-Simpson, telah disimulasikan secara rawak berikutan konsep teknik simulasi Monte-Carlo, yang kemudiannya akan digunakan pada keluk keruntuhan kutub pengedaran berdasarkan kelas kutub NESC. Selanjutnya, daya tahan infrastruktur kemudian dimodelkan dan dinilai dengan menggunakan 3 konsep penilaian daya tahan yang berbeza. Akhirnya, penilaian serta akan dilakukan untuk membanding ciri-ciri ketiga-tiga konsep penilaian daya tahan.

ACKNOWLEDGEMENTS

A debt of gratitude to all those who have contributed and made this project possible.

I would first like to express my most sincere appreciation to my supervisor, Professor IR. Dr. Hazlie Bin Mokhlis, for his generous commitment and dedication towards this project. I am humbled and gratefully indebted to his invaluable guidance.

I would also like to thank Associate Professor Suhail Afzal, for steering me into the right direction on countless occasions, and his promptness at any time of the day. I am truly gratified by his kind patience and consistent support.

Not forgetting, I must express my utmost gratitude to my family and friends, for the unconditional support throughout this period. Thank you for your contributions.

Lastly, I want to thank the University of Malaya for lending me its facilities which I required to complete this project. I made the decision to pursue my postgraduate program many years back, and I have not regret this decision ever since.

TABLE OF CONTENTS

Abstract	iii
Abstrak	iv
Acknowledgements	1
Table of Contents	2
List of Figures	5
List of Tables.....	7
List of Appendices	9
CHAPTER 1: INTRODUCTION.....	10
1.1 Background of Study	10
1.2 Problem Statement.....	10
1.3 Research Objective	11
1.4 Scope of Study.....	12
1.5 Report Outline	13
CHAPTER 2: LITERATURE REVIEW.....	15
2.1 Introduction.....	15
2.2 Power Systems in General	15
2.2.1 Transmission Networks	16
2.2.2 Distribution Networks	17
2.2.3 Distribution Networks	17
2.2.4 Challenges	19
2.2.4.1 Cyber-Attacks.....	19
2.2.4.2 Geomagnetism and Space Weather	20
2.2.4.3 Weather on Earth.....	21

2.3	Extreme Weather: A High-Impact, Low-Probability Event	22
2.3.1	Impact of Extreme Weather on Power Systems	23
2.4	Reliability in Power System	26
2.4.1	Reliability Assessment	28
2.5	Resilience in Power System.....	28
2.5.1	Methods to Evaluate Resilience	31
2.5.1.1	Qualitative Methods	32
2.5.1.2	Quantitative Methods	33
2.5.2	Summary of Common Qualitative and Quantitative Methods	34
2.5.3	Resilience Trapezoid	35
CHAPTER 3: METHODOLOGY.....		38
3.1	Introduction.....	38
3.2	Failure Probability	38
3.3	Power Flow and Radial Power Flow	44
3.4	Modelling a Stochastic Hurricane Storm.....	45
3.5	Timeline of Hurricane Storm Event	52
3.6	Process Flow Chart.....	52
3.7	Resilience Assessment.....	53
3.7.1	Resilience Triangle.....	54
3.7.2	Resilience Trapezoid	56
3.7.3	Code-Based Resilience Metrics.....	59
CHAPTER 4: RESULTS AND DISCUSSIONS		62
4.1	Introduction.....	62
4.2	Results from MATLAB Simulation	62
4.2.1	Base Value: 33-Bus Distribution System's Steady State	62

4.2.2	Simulation of Hurricane Storm and Pole Failure	64
4.2.3	Operational Functionality	66
4.2.4	Infrastructural Functionality	68
4.3	Evaluating the 33-Bus Distribution System with the Resilience Triangle Metrics 70	
4.3.1	Operational Functionality and Resilience	70
4.3.2	Infrastructural Functionality and Resilience	73
4.4	Evaluating the 33-Bus Distribution System with the Resilience Trapezoid Metrics 76	
4.4.1	Operational Functionality and Resilience	76
4.4.2	Infrastructural Functionality and Resilience	79
4.5	Evaluating the 33-Bus Distribution System with the Code-Based Resilience Metrics	83
4.5.1	Operational Functionality and Resilience	83
4.5.2	Infrastructural Functionality and Resilience	85
4.6	Evaluation of the Resilience Assessment Methods	86
4.6.1	Evaluation of the Resilience Triangle Assessment Method	86
4.6.2	Evaluation of the Resilience Trapezoid Assessment Method	88
4.6.3	Evaluation of the Code-Based Resilience Metrics Assessment Method	92
4.6.4	Summary of Evaluation	93
CHAPTER 5: CONCLUSION.....		94
5.1	Closing Summary	94
5.2	Future Works	95
	References	96
	Appendix	101

LIST OF FIGURES

Figure 2.1: Segregation of resilience component pre-event, during event, and post-event.	30
Figure 2.2: Qualitative methods in assessing resilience.....	33
Figure 2.3: Quantitative methods in assessing resilience.....	34
Figure 2.4: Summary of common qualitative and quantitative methods.	35
Figure 2.5: A generic resilience trapezoid.	36
Figure 3.1: A generic fragility curve.....	41
Figure 3.2: Fragility curves in reference to NESC pole class 2, 3, and 5, as simulated by MATLAB.....	43
Figure 3.3: An IEEE 33-bus radial distribution system.....	44
Figure 3.4: Defining the number of poles and iterations in MATLAB.	47
Figure 3.5: Defining the matrix of each NESC pole class in MATLAB.	48
Figure 3.6: Generation of random hurricane categories for each pole.....	49
Figure 3.7: Generating random 3-second gust speeds based on the randomly generated hurricane categories in MATLAB.	49
Figure 3.8: Generating failure probability for each NESC pole class.....	50
Figure 3.9: Process flow in generating failure probabilities with respect to the randomly generated hurricane gust speeds.....	51
Figure 3.10: Timeline of hurricane storm event.....	52
Figure 3.11: Flow chart of the evaluation of resilience assessment methods	52
Figure 3.12: A generic resilience triangle.....	54
Figure 3.13: The $\Phi\Lambda E\Pi$ metrics of the resilience trapezoid.....	57
Figure 3.14: Resilience variable with corresponding event duration in orders of 10.	60
Figure 4.1: Execution of “runpf.m” in MATLAB’s command window.....	62

Figure 4.2: 33-bus distribution system’s operational functionality and resilience with NESC pole class 2 ratings.	70
Figure 4.3: 33-bus distribution system’s operational functionality and resilience with NESC pole class 3 ratings.	71
Figure 4.4: Figure 4.4: 33-bus distribution system’s operational functionality and resilience with NESC pole class 5 ratings.	71
Figure 4.5: 33-bus distribution system’s infrastructural functionality and resilience with NESC pole class 2 ratings.	73
Figure 4.6: 33-bus distribution system’s infrastructural functionality and resilience with NESC pole class 3 ratings.	74
Figure 4.7: 33-bus distribution system’s infrastructural functionality and resilience with NESC pole class 5 ratings.	74
Figure 4.8: 33-bus distribution system’s operational functionality and resilience with NESC pole class 2 ratings.	76
Figure 4.9: 33-bus distribution system’s operational functionality and resilience with NESC pole class 3 ratings.	77
Figure 4.10: 33-bus distribution system’s operational functionality and resilience with NESC pole class 5 ratings.	77
Figure 4.11: 33-bus distribution system’s infrastructural functionality and resilience with NESC pole class 2 ratings.	80
Figure 4.12: 33-bus distribution system’s infrastructural functionality and resilience with NESC pole class 3 ratings.	80
Figure 4.13: 33-bus distribution system’s infrastructural functionality and resilience with NESC pole class 5 ratings.	81
Figure 4.14: Critical information disregarded by the resilience triangle assessment method.	87
Figure 4.15: Most-left Triangle in Resilience Trapezoid.	89
Figure 4.16: Center Rectangle in Resilience Trapezoid.	90
Figure 4.17: Most-right Triangle in Resilience Trapezoid.	91

LIST OF TABLES

Table 1.1: The selected resilience assessment methods.....	12
Table 2.1: Distribution network types.....	17
Table 2.2: Examples of quantities used to measure energy consumption.....	18
Table 2.3: Categories of high-impact, low-probability events.....	23
Table 2.4: Comparison between outages due to extreme weather and typical outages. .	24
Table 2.5: Types of extreme weather events.....	25
Table 2.6: High-level comparison between the concepts of reliability and resilience....	29
Table 2.7: Proposed resilience components and enhancing elements.....	31
Table 2.8: The resilience trapezoid phases.	36
Table 2.9: Proposed resilience trapezoid metrics.	37
Table 3.1: The Saffir-Simpson hurricane scale.....	39
Table 3.2: 3-second gust speeds for all hurricane categories in the Saffir-Simpson hurricane scale.....	40
Table 3.3: NESC pole class parameters.	42
Table 3.4: MATLAB M-Files from MATPOWER.	45
Table 3.5: Logic used to generate random gust speed based on hurricane category.	50
Table 3.6: The resilience triangle metrics.	55
Table 3.7: Mathematical expression of the resilience triangle metrics.	55
Table 3.8: The $\Phi\Lambda\Pi$ metrics of the resilience trapezoid.	58
Table 3.9: Mathematical expressions of each phase within the resilience trapezoid.....	59
Table 3.10: The code-based resilience metrics resilience categories.	60
Table 4.1: Power flow data of the 33-bus radial distribution system.....	63
Table 4.2: MATLAB simulated hurricane category and pole failure probability.....	64
Table 4.3: Indication of pole status	65

Table 4.4: Total disconnected load (MW) of each NESC pole class.....	66
Table 4.5: Generic measurement of the 33-bus distribution system’s operational functionality levels.....	67
Table 4.6: Total broken poles of each NESC pole class	68
Table 4.7: Generic measurement of the 33-bus distribution system’s infrastructural functionality levels	69
Table 4.8: Operational resilience triangle metrics of the 33-bus distribution system for NESC pole class 2, 3, and 5.	72
Table 4.9: Infrastructural resilience triangle metrics of the 33-bus distribution system for NESC pole class 2, 3, and 5.	75
Table 4.10: The operational $\Phi\Lambda E\Pi$ resilience trapezoid metrics of the 33-bus distribution system for NESC pole class 2, 3, and 5.....	78
Table 4.11: The operational resilience loss of the 33-bus distribution system for NESC pole class 2, 3, and 5	78
Table 4.12: The infrastructural $\Phi\Lambda E\Pi$ resilience trapezoid metrics of the 33-bus distribution system for NESC pole class 2, 3, and 5.....	81
Table 4.13: The infrastructural resilience loss of the 33-bus distribution system for NESC pole class 2, 3, and 5.	82
Table 4.14: Necessary variables for the assessment of the 33-bus distribution system’s operational functionality and resilience.	83
Table 4.15: The code-based resilience metrics for the operational functionality and resilience of the 33-bus distribution system for NESC pole class 2, 3, and 5.	84
Table 4.16: Necessary variables for the assessment of the 33-bus distribution system’s infrastructural functionality and resilience.....	85
Table 4.17: The code-based resilience metrics for the infrastructural functionality and resilience of the 33-bus distribution system for NESC pole class 2, 3, and 5	85
Table 4.18: Resilience variable categorization.	92
Table 4.19: Summary of evaluation.	93

LIST OF APPENDICES

Appendix A: MATLAB code of “case33bw.m” for 33-bus distribution system power flow data	101
Appendix B: MATLAB code of “runpf.m” to execute load flow analysis	104
Appendix C: Simulated power flow data of 33-bus distribution system	112
Appendix D: MATLAB coding written to generate random hurricane category and failure probabilities of poles in accordance to NESC pole class 2, 3, and 5.....	115
Appendix E: MATLAB output of random hurricane category and failure probabilities of poles in accordance to NESC pole class 2, 3, and 5	117

CHAPTER 1: INTRODUCTION

1.1 Background of Study

Power systems are undoubtedly the backbone to the modern-day society. It is hard to imagine the losses should any of these critical infrastructures fail even for a brief moment. Therefore, to increase the operational robustness, power systems have conventionally been designed and built with key principles involving concepts such as reliability, security, and adequacy. While these concepts are sufficient to mitigate and dampen regular occurrences that could cause disruptions in a power system's operations, newer, larger, and more sophisticated threats are now catching up to these conventional concepts.

Today more than ever, the ways of the modern society are steadily encouraging climate change, paving way for disastrous catastrophes at larger scales and higher frequencies. This presents a challenge to the reliability concept which does not prepare the conventionally designed and built power infrastructures in the face of large-scaled weather events. Thus, this leads the present-day engineers to explore a relatively new concept termed – “resilience”, to address the necessities for critical infrastructures such as power systems, to adapt to irregular catastrophic events.

As the concept is relatively new, further investigation is required on the definition of resilience and how it can be applied to evaluate the performance of power systems which could lead to identifying areas in need of enhancements, thus allowing power systems to adapt and to be well-prepared in the event of future disastrous events regardless of whether such events are weather-induced or man-made.

1.2 Problem Statement

There are subtle differences in the many research contributed to the current existing body of knowledge on the definition of resilience, thus leading to different evaluation

techniques and various metrics which ultimately results in a variance of modelling approaches and resilience enhancement methodologies.

While most of the recent studies address the need to conceptualize and quantify resilience, there are only a handful of studies with emphasis on the specific application of resilience assessment metrics for power systems impacted by disruptive and disastrous events. Without studies focusing on the area of application of such assessment metrics, the resilience of power systems cannot be evaluated and therefore mitigation and enhancement strategies cannot be planned, designed, and ultimately be implemented.

Finally, while there are studies proposing different types of resilience assessment metrics and frameworks, the lack of work carried out to compare the various resilience metrics and the attributes of each is evident.

1.3 Research Objective

The primary objective of this study is to evaluate the different power system resilience assessment methods and to summarize the attributes of each of the selected methods. The goals of this study can be expressed as shown in the below.

- i. To model a hurricane storm with categorized windspeeds and gust speeds based on the Saffir-Simpson's hurricane scale.
- ii. To develop three fragility curves in respect to the parameters of NESC pole class 2, 3, and 5.
- iii. To simulate failure probability of an IEEE 33-bus distribution system's distribution poles using the simulated hurricane gust speeds and fragility curves as variables.

- iv. To evaluate resilience assessment methods (resilience triangle metrics, resilience trapezoid metrics, code-based resilience metrics) through the application of the methods on the IEEE 33-bus distribution system.

1.4 Scope of Study

The topic of resilience is relatively new in comparison to topics such as reliability, security, and adequacy. As such, there is a limited amount of work proposing different types of resilience assessment methods and frameworks. Upon reviewing a substantial amount of literature, it is found that the “Resilience Trapezoid” framework recurs more frequently than other assessment frameworks and therefore is selected as a primary assessment method in this paper. Additionally, the resilience trapezoid is selected due to its straightforward approach which can easily be adapted for the case study in this work. However, in the interest of the main objective in this research, 2 other complementary resilience assessment methods are selected for comparison purposes, and along with the resilience trapezoid, are as listed in Table 1.1. Similarly, the selection of the additional assessment methods is due to the feasibility in applying to the case study.

Table 1.1: The selected resilience assessment methods.

No.	Assessment Method	Description	Adapted from
1	Resilience Trapezoid	Primary assessment method	(Panteli, Mancarella, Trakas, Kyriakides, & Hatzargyriou, 2017)
2	Resilience Triangle	Complementary assessment method (comparison purposes)	(Tierney & Bruneau, 2007)
3	Code-Based Resilience Metrics	Complementary assessment method (comparison purposes)	(Chanda, Srivastava, Mohanpurkar, & Hovsopian, 2018)

A load flow analysis will be carried out in this study to obtain the steady state values of the IEEE 33-bus distribution system, which will then be used as the base data. The assumption made here is that the distribution system is constantly in a steady state prior to the occurrence of a disastrous event, in which in this study, a hurricane storm. The windspeeds and gust speeds of the hurricane storm is generated randomly to mimic to stochastic behaviour of a natural disaster. Then, the fragility curves of the 33-distribution system's poles are modelled based on the NESC pole class 2, 3, and 5 parameters. The fragility curves represent the mechanical and tensile strength of the distribution poles, while also setting the functionality boundaries of each pole, and will be tested against the simulated hurricane storm. All modelling and simulation work will be carried out by the MATLAB software. Once the failed distribution poles have been identified, the system will be evaluated with the 3 selected resilience assessment methods. Then, the approach and attributes of each of the resilience assessment method will be evaluated, compared against each other, and summarized before a conclusion is drawn.

1.5 Report Outline

In summary, this study consists of 5 chapters, with each chapter dedicated to specific areas. In Chapter 1: Introduction, a brief preliminary is presented to highlight the goals and objectives of this research, and most importantly to establish the general need to investigate further on the topic of power systems resilience. Subsequently, in Chapter 2: Literature Review, past studies on the subject of power systems resilience, and resilience assessment methods are presented to reflect the volume of work in the existing body of knowledge. In the next segment, Chapter 3: Methodology aims to deliver the method of execution and how the works were carried out to achieve the goals and objectives on this research, before the simulated data is discussed and evaluations are made for each resilience assessment method in Chapter 4: Results and Discussion. Lastly, the research

is finalized in Chapter 5: Conclusion, whereby the evaluation carried out on each of the resilience assessment methods and their metrics, are concluded and prospective work for the future is proposed.

University of Malaya

CHAPTER 2: LITERATURE REVIEW

2.1 Introduction

Recent years have shown an increase in the contribution to the body of knowledge pertaining to the subject of resilience in power systems. The increasing emphasis on the subject is a reflection of a growing interest on how power systems can be buffered to withstand and perhaps avoid high-impact, low-probability catastrophic events that may cause damage to power systems and grids alike. While the general consensus points to the need for power infrastructures to be more resilient towards events driven by extreme weather conditions, the discussion point should be focused on refining the definition of a power system's resilience, and then extended to how resilience can be measured and quantified, in order for enhancements to be benchmarked and visualized.

2.2 Power Systems in General

Electricity has become a fundamental necessity in our modern society. In order for our community to function conveniently, electricity has to be generated from power infrastructures and generation plants. Hence, electrical power systems are now inseparably woven into the fabric of our civilization.

Conventionally, power generation plants are built quite a distant away from the load, more so for large-scale generation plants. This results in the generated power having to be siphoned from power plants over substantial distances before it reaches the end users. As such, intermediary infrastructures such a transmission and distribution networks come into the picture, enabling electricity to be dispersed to the end users. Ultimately, the main distinction between transmission and distribution networks is the voltage level of the electricity funnelling through each of these networks. The following segments will attempt to elaborate in general, the critical infrastructures of every power system.

2.2.1 Transmission Networks

A transmission network refers to the transfer of power from a generating source, very likely in the form of a power generation plant, to load centres whereby electricity is consumed commercially, industrially, and residentially. As mentioned in the earlier segment, generation plants are usually situated far from the load centre, thereby making distance a factor. The next crucial factor involves the economics of power generation, transmission, and distribution. Although from an economic standpoint, it is more efficient to generate power at low voltages, it is not financially feasible to transmit power at low voltages, more so over long distances.

Power generation plants typically produce voltages within the range of 11kV to 33kV. To reduce the power losses during transmission, the generated voltage is then stepped up to the transmission voltage. The transmission voltage level is dependent on transmission distance and is typically 132kV and above. The longer the distance, the higher the transmission voltage level should be to compensate losses. Additionally, transmission networks may also be categorized as the following.

i. Main Transmission Network:

Transmits to wholesale power outlets at 132kV and above

ii. Sub-Transmission Network:

Transmits power to retail power outlets at the range of 115 ~ 132kV

In short, transmission networks economically deliver power to outlets by stepping up the low-voltage power generated at generation plants.

2.2.2 Distribution Networks

Distribution networks can be viewed as systems delivering low-voltage power to the end users, by stepping down the stepped-up high-voltage power from the transmission networks connected to it. Power is channelled through a final step-down transformer to lower voltages to below 132kV before it can be utilized.

Other than the defining difference in voltage levels, distribution networks are distinctive from transmission networks particularly in terms of structure and topology. For one, distribution networks have a higher number of sources and branches in comparison to transmission networks. Additionally, most conventional distribution systems would include an on-load, tap-changing step-down transformer, distributing a wide network of circuits varying in length and varying loads on the other end connected to these circuits. Depending on the configuration and pattern, distribution networks can be divided primarily into 3 types, as shown in Table 2.1.

Table 2.1: Distribution network types.

Network Type	Characteristics
Radial Network	Cheapest to construct.
	Only one power source supplying to a group of end users.
	Failure would interrupt power for the entire network.
Circular Network (Ring)	Loops through a group of end users, before returning to original point.
	Usually has two power sources.
	Possible to supply power in both directions.
Mesh Network (Cluster)	Most complicated to construct.
	Most expensive to construct.
	Most reliable.

2.2.3 Distribution Networks

In general, there are 3 significant sectors that make up majority of the consumption of power generated as stated in the following page.

- i. Industrial Sector
- ii. Residential Sector (domestic)
- iii. Commercial Sector

While growing concerns over impact of energy on the environment has stimulated initiatives involving energy conservation and load management, with continued development and expansion, demand from the sectors above will very likely result in an increment in energy consumption. In general, the quantities utilized to measure the energy consumption can be expressed as shown in Table 2.2.

Table 2.2: Examples of quantities used to measure energy consumption.

Types	Description
Demand Estimation	Demand or load, at the receiving terminal, averaged over a fixed time interval, whereby Maximum Demand is the peak point of consumption.
	Time interval could vary depending on the region (15 mins / 30 mins / 60 mins).
Demand Factor	Ratio of Maximum Demand over all connected loads.
	Since it is highly unlikely for all connected loads to be running at maximum loads, ratio is usually less than 1.0 (0.8~0.95).
Load Factor	Ratio of Average Load over Maximum Demand, over a fixed time interval.
	Load Factor at 1.0 or unity, indicated that load is always drawing constant power without fluctuation.
Coincidence Factor	Ratio of Maximum Demand of incoming circuit to Total Maximum Demand of outgoing circuit.
	Coincidence Factor is dependent on the number of outgoing circuits.
	Demand of each outgoing circuit connected to the incoming circuit may vary.

2.2.4 Challenges

Due to the complexity of power systems, interruptions can be triggered by various sources including both natural and man-manufactured events (Borges Hink, Beaver, & Buckner, 2014). Contemporary studies based on real-world occurrences have shown the inability of power systems in delivering reliable and uninterruptible service due to network failures caused by both physical and cyber damage (Pasqualetti, Dorfler, & Bullo, 2011). This segment will briefly discuss some of the challenges faced by power systems.

2.2.4.1 Cyber-Attacks

In order to efficiently and intelligently deliver power to the consumers, the concept of “Smart Grid” has now emerged, integrating computer-based remote control, automation, and sophisticated bidirectional communication technology into power systems. In short, power grids are now accessible, whether directly or indirectly, via the Internet.

With the integration of cyber system, power systems are now more efficient, bringing about a string of benefits such as stability, reliability, and flexibility in the especially in the managing of operations and control (Anwar & Mahmood, 2014). Packaged with communication networks such as SCADA and Advanced Metering Infrastructure, data from remote and isolated power facilities can be monitored, collected, and measured while control commands may also be communicated bidirectionally (Esfahani, Vrakopoulou, Margellos, Lygeros, & Andersson, 2010). However, this layer of communication, with all its merits, is susceptible to cyber-attacks.

The two-way information flow model in which the Smart Grid operates fundamentally on, is susceptible to a few potential risks, mainly in the areas of data privacy and entry points as described in the following page.

i. Data Privacy

With the capacity and the increased frequency in data flow, confidentiality is compromised, and the risk of customer privacy breach is glaringly present.

ii. Potential Entry Points

Entry points, vulnerable and easily accessible to cyber-attacks, increases with the expansion of the grid network as every node becomes a potential intrusion point for malicious cyber-attacks.

The growing population of technologically savvy cyber terrorists in this day and age, have resulted in a drastic incline in the number of cyber-attack related cases, threatening the integrity and confidentiality of the information embedded in power systems (Anwar & Mahmood, 2014). Without the appropriate prevention and mitigation procedures, cyber-attacks can induce catastrophic damage to the likes caused by extreme weather events (Borges Hink, Beaver, & Buckner, 2014). Therefore, power systems must be equipped with the appropriate software, hardware, and skilled personnel to protect and prepare against any form of cyber-attacks.

2.2.4.2 Geomagnetism and Space Weather

Geomagnetic storms are a result of the Earth's magnetic field capturing ionized particles from solar wind flares caused by coronal mass ejections by the Sun (Kappenman J. , 2010). When such disturbances occur, the geoelectric field at the surface of the Earth directs the geomagnetically induced currents through networks with the capacity to conduct electricity such as power systems, and oil and gas pipelines (Thomsom, McKay, Clarke, & Reay, 2005). With the continual growth of power system infrastructures, the

disturbances caused by geomagnetic events may cause large-scale damage on power grids.

Transformers with grounded neutrals installed at power grids that are exposed to such events, conveniently provide a path from networks affected by geomagnetic events, to ground (Horton, Boteler, Overbye, Pirjola, & Dugan, 2012). Thus, the geomagnetically induced currents generated end up saturating the magnetic core of these exposed transformers. This results in the distorted and large AC currents being drawn from the power grid. In the event of a geomagnetic event on a large network of interconnected power grids, concurrent injections of such amplified and distorted AC currents may increase reactive power demands that result in voltage regulation issues.

Additionally, such distorted AC currents when introduced into the network, may disrupt the performance of other connected apparatuses, resulting in off-line trips (Schrijver & Mitchell, 2013). Lastly, transformers that are exposed to such events, operate at nonlinear saturation range, risking overheating and subsequently permanent damage (Kappenman J. G., 2004). While there are technical and operational workarounds to the risks associated with geomagnetic induced currents on power systems, the inclining trend to expand power networks and to increase interconnections between, as well as the continued utilization of high-voltage, low resistance systems, such risks cannot be completely eradicated (Thomsom, McKay, Clarke, & Reay, 2005).

2.2.4.3 Weather on Earth

In the recent years, a radical change is observed in global weather. Rising temperature are melting ice caps and mountain glaciers, accelerating the rise of sea level and ocean acidity (Fogarty & Tan, 2019). Along with this comes the unpredictability and the

changes in seasonal rainfall patterns, very likely due to an increased moisture content captured by a warmer atmosphere (Clark, 2011).

As our demand for energy continues to grow, changes in the load patterns can be related to the imposing of operational stress on power systems and both its infrastructure and apparatuses, revealing higher vulnerabilities in faults and breakdowns (Kezunovic, Dobson, & Dong, 2008). Simply put, rising temperatures will increase power consumption and raise the power demand peak, while reducing the lifespan of transformer due to constant operation at maximum capacity (Shahid, 2012). Furthermore, the component ratings of a power system can be affected by external parameters such as the surrounding ambient temperature and wind speeds, reducing overall power generation, transmission, and distribution efficiency (Michiorri & Taylor, 2009).

In addition to the evolving load demand caused by climate change, power systems are also vulnerable to physical damage caused by environmental conditions induced by unfavourable weather. Transmission and distribution systems consist of overhead and underground infrastructures and facilities whereby when physical stresses caused by extreme wind speeds, lightning strikes, icing, and so on, are introduced to these systems during bad weather, result in component failure and subsequently, disruption in power supply service (Billington, Wu, & Singh, 2002).

2.3 Extreme Weather: A High-Impact, Low-Probability Event

An extreme weather event, unlike typical bad weather, is a weather event with inputs of destructive variables and factors that often lead to disastrous impacts that are catastrophic, unpredictable, unseasonal, and historically extreme (Abi-Samra & Malcolm, 2011). Globally, extreme weather events in the form of natural disasters, such as windstorms, hurricanes, cyclones, tsunamis, severe floods, and earthquakes, have

displayed cataclysmic levels of impact on not only the infrastructure and economy, but the general public's health and safety as well.

A high-impact, low-probability event is a hazardous event with the capacity to produce devastating effects. By virtue of their rare occurrences however, high-impact, low-probability events happen at low frequency. Extreme weather hazards in the form of natural disasters, are considered as high-impact, low-probability events, and may result in devastating consequences on critical infrastructures. While the severity of the outcome of each event is unknown, what is predictable is that the likelihood of the frequency and the impact of these events will increase in the near future given the current situation with climate change (Espinoza, Panteli, Mancarella, & Rudnick, 2016).

As shown in the below, Table 2.3 indicates the many examples of hazardous events that are categorized as high-impact, low-probability events (Veeramany, et al., 2016).

Table 2.3: Categories of high-impact, low-probability events.

Category	Examples
Natural disaster	Meteorological: Hurricane, tornado, snowstorm
	Geological: Seismic activity, volcanic activity
	Hydrological: Flood
	Space Weather: Geomagnetic storm
Biological hazards	Biological: Pandemic events
Unintentional human hazards	Operational mistake
	Operational mishandling
Malicious human hazards	Physical attack, vandalism, cyber-attack, electromagnetic pulse

2.3.1 Impact of Extreme Weather on Power Systems

The consequences of extreme weather events on power systems are becoming convincingly evident globally in the recent years (Panteli, Mancarella, Trakas, Kyriakides, & Hatziargyriou, 2017). With the initiation of an extreme event, the interruption caused by the failure of one grid could have potential cascading effects, leading to the increase in loads for other grids or even further interruptions due to the

reduced ability to execute time-sensitive corrective measures (Veeramany, et al., 2016). Electricity is required to drive the backbone of our society which includes critical infrastructures such as transportation, communication, food production and supplies, water treatment and supply, and health systems. Therefore, interruptions that disrupt the continuous supply of electricity would result in drastic consequences. In addition to the high impact, interruptions are likely to be sustained in duration, spanning from hours to days, because of the damage across large portions of the network (Panteli & Mancarella, 2015). While scholars have placed emphasis on this, the reality is that continuous supply of electricity without disruptions is close to impossible due to the many threats that power systems are exposed to. Generally, these threats come in the form of typical threats, and threats caused by high-impact, low-probability events such as a catastrophic natural disaster. Table 2.4 is a summary of comparison points between outages due to extreme weather events and typical outages. (Panteli & Mancarella, 2015).

Table 2.4: Comparison between outages due to extreme weather and typical outages.

Typical Power System Outage	Outage due to Extreme Weather
Low-impact, high-probability	High-impact, low-probability
Likely to be predictable, thus easier to control and mitigate	Unlikely to be predictable, thus difficult to control and mitigate
Location and time of occurrence is random	Spatiotemporal correlation between faults and event
Contingency and mitigation analysis tools can be utilized to predict, monitor, and control event	Unpredictable event
Lesser number of faults	Larger number of faults
Network is largely intact	May expect a large portion of the network to suffer damage and breakdown
Restoration is easier and quicker	Restoration is time and resource consuming.

As introduced in earlier segments, the impact of extreme weather conditions severely affects critical infrastructures. Power systems are undoubtedly as essential as any other critical infrastructures as it is irrefutably the backbone of this technologically driven society and therefore may also come under the adversely negative impact of catastrophic weather events (Panteli, Pickering, Wilkinson, Dawson, & Mancarella, 2017). As a significant threat to the safety and reliability of a power system's operations, extreme weather events have the potential to cause adverse losses to the grid (Li, Xie, Wang, & Xiang, 2019). Table 2.5 is a summary of the damages that extreme weather events may cause onto power systems.

Table 2.5: Types of extreme weather events.

Types	Description
Floods	May cause lasting damages due to flood water.
	May be grouped as:
	1) Flash floods 2) River floods
	Flash floods typically cause the most damage due to heavy downpours that result in water surges that can damage infrastructures and block roads and pathways.
	Flood water can cause rust, and entrap mud, and debris, which makes repair and restoration works in a substation difficult.
Windstorms	May be grouped as:
	1) Synoptic winds 2) High-intensity winds
	May not necessarily come with precipitation.
	Causes physical damage to power infrastructures due to strong gusts of high-velocity winds.
	May cause power lines to swing in a volatile manner, resulting in fault or short-circuiting.
	Severe gusts may break utility lines and poles.
Tropical Storms (E.g. Hurricanes)	Causes intense winds and flooding.
	Effects are similar to those of floods and windstorms.
	Loses intensity as hurricanes move across the land.
Blizzards & Snowstorms	Intense winds accompanied by snowfall.
	Effects are similar to those of windstorms.

	Additionally, snow deposits on power lines, may cause the lines to break.
Earthquake	Quake with substantial magnitude may physically damage equipment and infrastructure.
	Quake may also cause tsunamis and landslides, which can also lead to physical damage to power infrastructures.

Power outage events that have occurred in the recent decades have been studied amply and considerably by the society of engineers (Kundur, Taylor, & Pourbeik, 2007). Proposed solutions to minimize the effects of weather-induced outages include enhanced tree-trimming frequencies, underground installation of distribution and transmission lines, implementation of the Smart Grid concepts, and improving utility maintenance practices (Campbell, 2012). Despite the collective resources in the body of knowledge, there exists no concluding mitigation guidelines for extreme weather events. It is therefore unquestionably necessary to develop appropriate techniques and methods that can be utilized to systematically assess the shortcomings of power systems, that come under the influence of high-impact, low-probability events such as extreme weather conditions (Espinoza, Panteli, Mancarella, & Rudnick, 2016).

2.4 Reliability in Power System

Power system reliability is one of the most crucial discussion in the power industry as it brings about high impact in the commercial area of power generation most notably on the cost of electricity and end user satisfaction (Brown, 2008). In recent times, power systems have been introduced to the concept of integrating various renewable energy resources such as wind generation systems and photovoltaic systems, which brings about a new set of technical issues such as islanding, harmonics, et cetera ((Bouhouras, Marinopoulos, Labridis, & Dokopoulos, 2010).

The concept of reliability then, becomes an important method to measure a power system's ability to consistently deliver power in accordance to the demand of the end users. Briefly put, reliability of a power system can be expressed as the capability to deliver power to end customers with minimal to no interruptions (Sekhar, Deshpande, & Sankar, 2016).

As the growth and development of our society is tied to our demand for electrical power, rigorous expansion and construction of power systems is required in order for our society to operate. However, with an aggressive expansion rate, comes numerous issues pertaining to power quality, resulting from poorly planned technical designs of power systems (Sekhar, Deshpande, & Sankar, 2016).

Conventional power systems have always been designed with the classical concept of "Reliability". The key components of the concept of reliability can be broken down to two major categories.

- i. Adequacy

The availability of sufficient network capacity to guarantee supply of electricity on extended durations, without interruptions under normal operating and load demand conditions.

- ii. Security

The ability of an adequately designed network to withstand disturbances, without breaking supply.

Thus, the concept of reliability then, can simply be expressed as a design principle which tries to meet the day-to-day requirement of continuously supplying the end users

with high-quality power, and coping with substantial but common threats. The following segment will attempt to further elaborate on the concept of reliability.

2.4.1 Reliability Assessment

The reliability of an electrical power system is crucial to the convenience and security for all consumers, most notably in sectors – industrial, commercial, and residential (Ali, Wiyagi, & Syahputra, 2017). With heavy emphasis being placed on quality and continuity of power supply, various indices have been defined to assess the reliability and serviceability of power systems (Rosendo, Gomez-Exposito, Tevar, & Rodriguez, 2008).

- i. SAIFI: System Average Interruption Frequency Index

$$SAIFI = \frac{\text{Total No. of Customer Interruptions}}{\text{Total No. of Customer Served}} \quad (2.1)$$

- ii. SAIDI: System Average Interruption Duration Index

$$SAIDI = \frac{\text{Sum of All Customer Interruption Duration}}{\text{Total No. of Customer Served}} \quad (2.2)$$

- iii. CAIDI: Customer Average Interruption Duration Index

$$CAIDI = \frac{\text{Sum of All Customer Interruption Duration}}{\text{Total No. of Customer Interruptions}} \quad (2.3)$$

$$CAIDI = \frac{SAIDI}{SAIFI} \quad (2.4)$$

2.5 Resilience in Power System

While power systems engineering is considered to be one of the pioneering areas of electrical engineering, the pace of its technological and commercial revolution surpasses even the most modern of technologies (Brown, 2008). With the ever-growing demand for energy, power networks are expanding in size and complexity. However, as the world

witnesses extreme weather events occurring at a higher rate due to climate change, it is imperative for our critical infrastructures to be able to cope with the inclining radical weather patterns. Although security and adequacy, two components of reliability, have always been major concerns for future power systems with distributed generation, the constant evolution of the industry demands have deprioritized the relevance of these concepts. The concept of reliability then, though tried and true, may only be useful for achieving acceptable service quality. Taking into consideration, the rapidly changing environmental conditions which have been proven to impact the operation and performance of power systems, a more comprehensive and sophisticated method must be deployed to assess the risk associated with these systems. This new method or concept must cover not only conditions which are predictably normal, but also conditions which are extreme at random. As expressed in the previous segments, high-impact, low-probability events caused by weather, can lead to destructive outcomes and complete black-out of a power system. In the case of a critical power infrastructure, being struck by a weather-driven high-impact, low-probability event could potentially result in the electrical disconnection of thousands if not millions. As conventional power systems were designed and built to only be resistant towards common threats, a new concept is then necessary to address the arising issues of catastrophic events, hence the coining of a new principle in power systems – “Resilience”. Table 2.6 is a high-level comparison between the concepts (Panteli & Mancarella, 2015).

Table 2.6: High-level comparison between the concepts of reliability and resilience.

Reliability	Resilience
Low-impact, high-probability	High-impact, low-probability
Static and mostly unable to adapt	Adaptive, constantly changing
Assesses the state of power system (snapshot of a point in time)	Assesses the state and transitioning between states of power system
Prioritizes customer downtime	Prioritizes customer downtime and restoration time

The concept of resilience was first introduced as a method to assess the diligence of systems and their capacity to incorporate change and disruption while sustaining the same correlations between populations or state variables (Holling, 1973). As time wore on, the originally defined concept of resilience continued to evolve and along the way, was adopted by many, most notably in the areas of social-ecology, health and safety, organization, and economics (Panteli & Mancarella, 2015). In one study, resilience was expressed as possessing the capacity to “anticipate, absorb, adapt to and/or rapidly recover from a disruptive event”, whereby the primary attributes of a resilient system should include resistance, redundancy, responsiveness, and recovery (Cabinet Office, 2011). In line with this, conceptual resilient frameworks have also proposed similar attributes such as robustness, redundancy, resourcefulness, and rapidity (Panteli & Mancarella, 2015). Similarly, another report suggests that resilience can be expressed as an entity having the capability to anticipate, resist, absorb, respond to, adapt to, and recover from a disruption, and therefore can be segregated into several components as shown in Figure 2.1 (Lin, Bie, & Qiu, 2018).

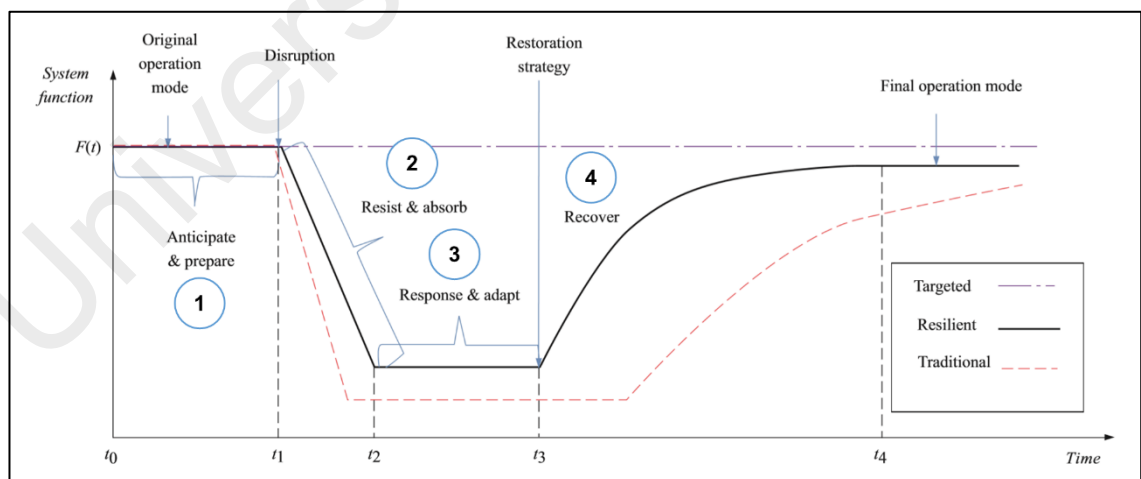


Figure 2.1: Segregation of resilience component pre-event, during event, and post-event.

Referring to Figure 2.1, each resilience component proposed can be enhanced with specific elements as proposed in Table 2.7 (Calrson, et al., 2012).

Table 2.7: Proposed resilience components and enhancing elements.

Enhancement	Component	Description
Readiness	Anticipate	Actions taken to define the disastrous/catastrophic event
Mitigation	Resist	Actions taken pre-event to cushion the severity and lessen the impact of the event
	Absorb	
Responsiveness	Respond	Actions taken immediately post-event to manage and control the impact of the event
	Adapt	
Restoration	Recover	Actions taken return and restore conditions to an acceptable state

While there is not a unanimous definition of what resilience is and should be, the general expression of its representation can simply be stated as a concept that encompasses a power system's operational performance and availability prior to, during, and after a high-impact, low-probability event (Bie, Lin, Li, & Li, 2017).

2.5.1 Methods to Evaluate Resilience

In the past, the concept of resilience has been approached by academicians and researchers from various viewpoints which includes the well-being of the society, engineering feasibility and scalability, and economics (Lin & Bie, 2016). There are societies and entities which include government bodies, institutes, and academicians, that have touted resilience as a beneficial concept that may help in the achieving of enormous savings by identifying and reducing risks, while also expediting restoration and recovery (Ayyub, 2014).

Studies have indicated that power systems are generally reliable but not necessarily resilient, and in order to preserve the continuity of supply, additional considerations that stretch beyond the conventional reliability analysis is necessary (Lin, Bie, & Qiu, 2018). While there are ample amount of studies and publications on the topic of resilience, most notably in the areas of its concept, a generic consensus on a universal measurement or assessment framework has yet to be concluded.

The existing body of knowledge on the study of resilience has mostly focused on defining and evaluating resilience. It is important to note that the evaluation of resilience can be deemed as the foundation of resilience enhancement. In addition to this, the existing works on the topic of resilience evaluation can be segregated into two silo of assessment methods – 1) qualitative, and 2) quantitative. A brief outline of each method is as shown in the following segments.

2.5.1.1 Qualitative Methods

Qualitative assessment methods generally serve as guidelines for defining energy policies and may provide only high-level aspects of assessed systems. While in varieties, common evaluation methods are usually presented in the form of surveys, checklists, rating scales, and questionnaires. There is also a study which introduced performance scoring matrices that subjectively evaluates different aspects of a system's resiliency (Roeger, Collier, Mancillas, McDonagh, & Linkov, 2014). In addition to these methods, a research work has proposed the utilization of analytic assessment for the purpose of assessing the system's function and resiliency, by comparing subjective opinions from various entities (Orencio & Fujii, 2013). Figure 2.2 as shown in the next page, is a summary of the qualitative methods mentioned (Bie, Lin, Li, & Li, 2017).

Qualitative Assessment Methods	
Aspects Assessed	Assessment Methods
<ul style="list-style-type: none"> ▪ Power Infrastructure ▪ Information system and network ▪ Business structure ▪ Etc. 	<p>[Survey]</p> <ul style="list-style-type: none"> ▪ Checklist ▪ Rating scales ▪ Questionnaire
<p>Capabilities Assessed</p> <ul style="list-style-type: none"> ▪ Readiness ▪ Prevention and mitigation ▪ Responsiveness ▪ Restoration and recover ▪ Etc. 	<p>[Matrix-based approach]</p> <ul style="list-style-type: none"> ▪ Performance metrics ▪ Performance matrixes ▪ Evaluate system function
	<p>[Analytic-based]</p> <ul style="list-style-type: none"> ▪ Analytic hierarchy process ▪ Evaluate comparable quantities

Figure 2.2: Qualitative methods in assessing resilience.

2.5.1.2 Quantitative Methods

Quantitative methods are usually deployed to measure and analyse quantifiable performance metrics and values such as load (connected and disconnected), and duration (interruption and restoration). Such performance measurements can be utilized to draw comparisons between the targeted performance and actual performance, thus enabling the effectiveness of systems to be evaluated. In addition to this statement, quantitative resilience measurements must be able to capture performance of each individual and specific interruptions and events, to assist in the process of decision making (Watson, et al., 2015). Figure 2.3 as shown in the next page, is a summary of some of the more common quantitative evaluation techniques (Bie, Lin, Li, & Li, 2017).

Quantitative Assessment Methods	
Simulation-based	▪ Resilience-measuring induced costs
	▪ Ratio between targeted and actual performance
	▪ Component connectivity based on complex-system method
Analytical Method	▪ Probability analysis on the system performance
Historical Statistics Analysis	▪ Duration of interruption to restoration
	▪ Rate of restoration

Figure 2.3: Quantitative methods in assessing resilience.

Of the methods shown in Figure 2.3, the simulation-based method, which incorporates catastrophic scenarios and post-event impact, is considered to be the most commonly utilized method applied to assess system resilience (Bie, Lin, Li, & Li, 2017). One example of the quantitative method that has been gaining traction amongst researchers, is the “Resilience Trapezoid (Panteli, Mancarella, Trakas, Kyriakides, & Hatziargyriou, 2017). Further details on the resilience trapezoid will be discussed in the following segments.

2.5.2 Summary of Common Qualitative and Quantitative Methods

To allow an appropriate assessment of the state of a system prior, during, and after a catastrophic event, and to evaluate the vulnerable areas, a quantitative method should be adopted to accurately measure the quantifiable metrics of the impact resulting from the catastrophic event (Dunn, Wilkinson, Alderson, Fowler, & Galasso, 2018). Therefore, the

focal point of this study will be carried out by employing quantitative methods, most notably the resilience trapezoid method. Figure 2.4 summarizes both quantitative and qualitative methods.

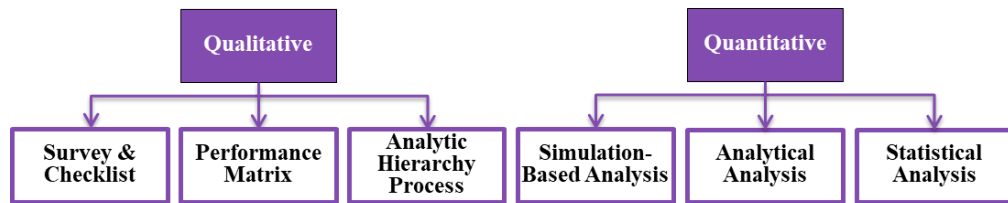


Figure 2.4: Summary of common qualitative and quantitative methods.

2.5.3 Resilience Trapezoid

In this segment, the concept of resilience trapezoid will be discussed further, with elaboration on the time-dependent metrics that define the various phases utilized to assess the resilience of a power system.

Figure 2.5 displays a generic resilience trapezoid along with its many phases, whereby the resilience indicators deployed to measure the resiliency of a system as an extreme event takes place, is indicated as a function of time (Panteli, Mancarella, Trakas, Kyriakides, & Hatziargyriou, 2017). To briefly expand on the topic, the resilience trapezoid may be deployed to assess the following.

i. Operational Resilience

The attributes of a power system that provide secure and stable operational and functional robustness.

ii. Infrastructural Resilience

The physical attributes notably robustness, of a power system to mitigate and withstand disastrous events.

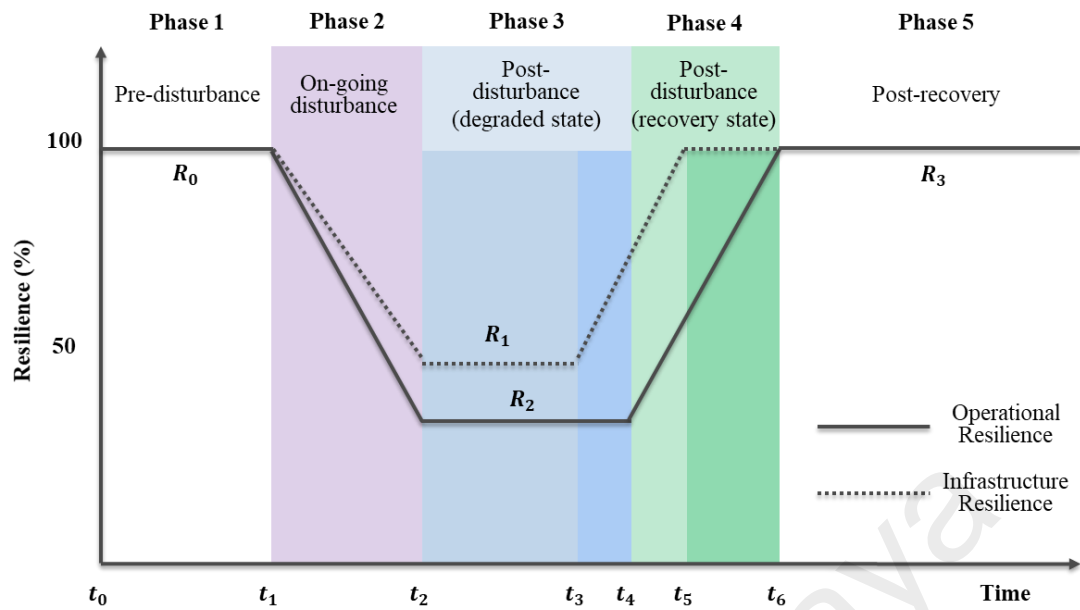


Figure 2.5: A generic resilience trapezoid.

As shown in Figure 2.5, the resilience of a system, can be assessed by the many phases of the resilience trapezoid, which each state uniquely represented by a state in which the system is undergoing. As shown in the below, Table 2.8 is a summary of each phase.

Table 2.8: The resilience trapezoid phases.

Phase	State	Description
1	Pre-disturbance (t_0 to t_1)	Event has not occurred therefore system is online and functioning at a normal state.
2	On-going disturbance (t_1 to t_2)	<p>> Infrastructure Resilience: Resilience level drops from R_0 to R_1</p> <p>> Operational Resilience: Resilience level drops from R_0 to R_2</p> <p>It should be highlighted R_1 and R_2 could differ, subject to the system and impact of the event, and therefore are system- and event-dependent.</p>
3	Post-disturbance degraded state (t_2 to t_4)	Event has ended, and system has completely degraded, pending recovery efforts. Restoration start time may be different for operation and infrastructure, subject to resilience solutions.
4	Post-disturbance recovery state (t_4 to t_6)	System recovery is on-going, and restoration is gradual. Similar to Phase 3, rate of restoration may be different for operation and infrastructure.
5	Post-recovery (t_6 onwards)	System has been restored, online, and functioning at a normal state.

In addition to defining the phases of a disruption-struck system, it is crucial to also define a set of metrics that enable the system's performance in each phase to be captured and utilized for the measurement of the system's resiliency. A recent study has proposed the “ $\Phi\Lambda E\Pi$ ” metrics along with the “trapezoid area” metric to help express the resilience trapezoid phases and states as shown in Table 2.9 (Panteli, Mancarella, Trakas, Kyriakides, & Hatziargyriou, 2017).

Table 2.9: Proposed resilience trapezoid metrics.

Phase	State	Metric	Description
2	On-going disturbance ($t1$ to $t2$)	Φ	Rate of functionality decline (how steep is gradient)
		Λ	Decline in functionality levels
3	Post-disturbance degraded state ($t2$ to $t4$)	E	Duration of post-disturbance degraded state (how long before restoration can begin)
4	Post-disturbance recovery state ($t4$ to $t6$)	Π	Rate of functionality recovery (how steep is gradient)
2-to-4	Post-recovery ($t1$ to $t6$)	Resilience Loss	Area of trapezoid which indicates loss of functionality and performance

To conclude, the resilience trapezoid and the $\Phi\Lambda E\Pi$ metrics as shown above, is an appropriately efficient quantitative method that can be deployed for the purpose of efficiently and systematically measuring the resilience of power systems. Thus, this chapter is now concluded. The following chapters and segments will attempt to demonstrate on how the methods introduced earlier can be utilized to evaluate the resilience of a power system.

CHAPTER 3: METHODOLOGY

3.1 Introduction

To carry out this study, quantitative assessment methods will be deployed. The resilience trapezoid introduced in the earlier chapter, will be utilized as the primary assessment method to evaluate the different stages that a selected power system network would undergo when struck by an extreme weather event in the form of a hurricane storm. Additionally, fragility curves that represent weather-dependent failure probabilities, along with windspeeds of different categories, will be integrated into this study to determine the failure of distribution poles. The distribution poles employed to simulate this study will be categorized based on the standards as set by the National Electrical Safety Code (National Electrical Safety Code, 2007). Lastly, as the base of the case study in this paper, a 33-bus radial distribution system will be used to illustrate the proposed methodology (Baran & Wu, 1989). All modelling of fragility curves and scenario testing of failure probabilities will be simulated by utilizing the MATLAB simulation program.

3.2 Failure Probability

As expressed in the earlier segment, the resilience of a 33-bus radial distribution system will be put to the test against a hurricane storm. In the case of overhead systems, power interruptions during hurricane storms typically occur due to trees snapping power lines, and intense winds blowing down poles (Ma, Chen, & Wang, 2018). To model the failure of distribution poles during a hurricane storm, the concept of fragility curve is introduced to indicate the failure probability of the distribution poles as a function of weather-based parameters such as windspeeds. Table 3.1 as shown in the next page, indicates the hurricane categories, according to the Saffir-Simpson hurricane scale (Schott, et al., 2010).

Table 3.1: The Saffir-Simpson hurricane scale.

Category	Windspeeds	Impact
1	74-95 mph (119-153 km/h)	<ul style="list-style-type: none"> >Poorly built homes will suffer major damage to roof and gable ends. >May cause damage to roof, vinyl sidings, and gutters of solidly built houses. >May break branches of trees. >May uproot and topple shallowly rooted trees. >May cause damage to power lines and poles that could potentially cause interruptions that could last several days.
2	96-110 mph (154-177 km/h)	<ul style="list-style-type: none"> >Poorly built homes will suffer major damage to roof and gable ends. >May cause major damage to roof, vinyl sidings, and gutters of solidly built houses. >Many shallowly rooted trees will be uprooted, causing roadblocks. >Near-complete power loss is likely with interruptions that could last from several days to weeks.
3	111-129 mph (178-208 km/h)	<ul style="list-style-type: none"> >Will cause catastrophic damage even to solidly built house, possibly dismantling the roof decking and gable ends. >Many shallowly rooted trees will be uprooted, causing roadblocks. >Even upon the settling of the storm, supply of electricity and water will be not be available for several days to weeks.
4	130-156 mph (209-251 km/h)	<ul style="list-style-type: none"> >Will cause catastrophic damage even to solidly built houses can sustain severe damage with the destruction of most of the roof structure and/or some exterior walls. >Many trees will be snapped or uprooted >Many utility poles will be downed. >Fallen trees and downed utility poles will block roads, contributing to the isolation of residential areas. >Power loss will sustain from weeks to possibly months.
5	>156 mph (>252 km/h)	<ul style="list-style-type: none"> >Will cause catastrophic damage - A large portion of solidly-built houses will be destroyed, with walls and roofs collapsing. >Most trees will be snapped or uprooted. >Most utility poles will be downed. >Fallen trees and downed utility poles will block roads, contributing to the isolation of residential areas. >Power loss will sustain from weeks to possibly months.

It has been proposed that windspeeds of category-1 and -2 are considered to be less destructive whereas windspeeds of category-3 and above have been classified as major hurricanes by the U.S. National Hurricane Centre (Eskandarpour, Khodaei, & Lin, 2016). Another study has proposed the “gust factor” which is the potential of each windspeed category to having 3-second gusts that have speeds estimated to be 25% faster than 1-minute sustained windspeeds (Brown R. , 2009). As it is typical for extreme wind ratings to be utilized for the design of utility structures, the gust factor is selected to be incorporated with the fragility curve when carrying out the case study in this paper. Table 3.2 indicates the windspeeds and gust speeds of all hurricane categories (Eskandarpour, Khodaei, & Lin, 2016).

Table 3.2: 3-second gust speeds for all hurricane categories in the Saffir-Simpson hurricane scale.

Category	1-Minute Sustained				3-Second Gust Speed			
	MPH		MPS		MPH		MPS	
	Min	Max	Min	Max	Min	Max	Min	Max
1	74	95	33	42	93	119	42	53
2	96	110	43	49	120	138	54	62
3	111	129	50	58	139	162	62	72
4	130	156	58	70	163	195	73	87
5	>156		>70		>195		>87	

As introduced earlier, the failure probabilities of the distribution poles will be simulated based on windspeeds and fragility curves. Referring to the below, there are several methods to derive the fragility curve.

- i. Statistically analysing a substantial set of data on failure occurrences
- ii. Experimental means – by intentionally causing failure
- iii. Analysis through simulation
- iv. Through acumen and “know-how” of subject matter experts
- v. Combination of any of the methods above

For the purpose of carrying out this study, the method deemed most resource appropriate would be analysis through the modelling of the fragility curve via simulation. Figure 3.1 displays a generic fragility curve.

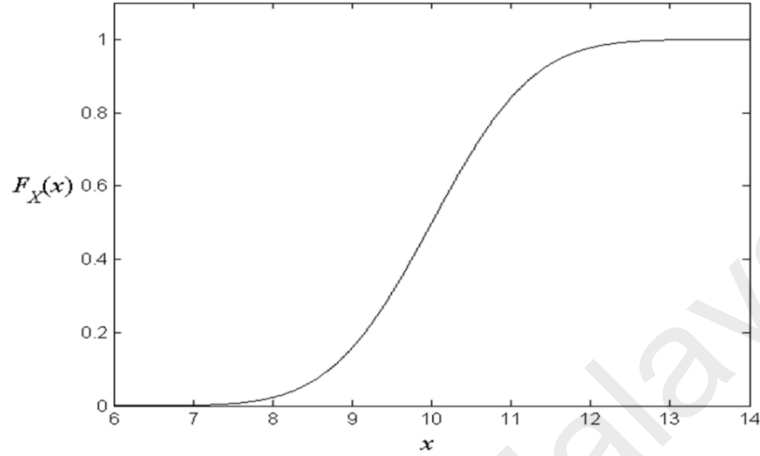


Figure 3.1: A generic fragility curve.

In this study, the fragility and structural damage tolerance of the 33-bus radial distribution system's distribution poles will be tested. Therefore, the structural integrity of the poles can be represented by the cumulative distribution function of a lognormal distribution. The mathematical model is as shown in the below (Panteli, Pickering, Wilkinson, Dawson, & Mancarella, 2017).

$$p = \varphi\left(\frac{1}{\sigma} \times \ln \frac{x}{\mu}\right) \quad (3.1)$$

Whereby,

φ = standard normal cumulative distribution function

x = 3 – second gust speed

μ = median of pole mechanical resistance

σ = standard deviation of pole mechanical resistance

To simulate the failure probabilities of the utility poles, the fragility curve that is represented by the lognormal cumulative distribution, will be modelled by utilizing MATLAB's "logncdf" function. The generic MATLAB command is as follows.

$$P = \text{logncdf}(X, MU, SIGMA) \quad (3.2)$$

Whereby in the case of this study,

$P = \text{failure probability of pole}$

$X = 3 - \text{second gust speed (intensified windspeed)}$

$MU = \text{median of pole mechanical resistance}$

$SIGMA = \text{standard deviation of pole mechanical resistance}$

The failure probability of a pole is dependent on the shape of the fragility curve, and the load imposed on the pole which is caused by the intensity of the windspeed. However, the shape of the fragility curve, is dependent on the parameters of the pole which would be the median and standard deviation of the pole's mechanical load resistance. The necessary pole parameters are adapted from another study (Ma, Chen, & Wang, 2018). In this study, 3 pole categories will be provided, thus, 3 fragility curves will be modelled by using MATLAB's "logncdf" function. The necessary pole parameters are based on the NESC pole classes and are as shown in Table 3.3 (Ma, Chen, & Wang, 2018).

Table 3.3: NESC pole class parameters.

NESC Pole Class	Mechanical Resistance	
	Median (μ)	Standard Deviation (σ)
2	5.05	0.135
3	4.94	0.140
5	4.76	0.137

As indicated in Table 3.3, 3 pole classes are available, therefore 3 different scenarios will be simulated. The median of each pole class represents the capability of the pole to absorb mechanical load. The higher the median value, the higher the capability to tolerate mechanical load, and thus the lower the failure probability. This is because the median value determines the position of the fragility curve. The higher the median, the further the fragility curve is pushed towards the right (failure at higher windspeeds). The simulated fragility curves are as shown in Figure 3.2.

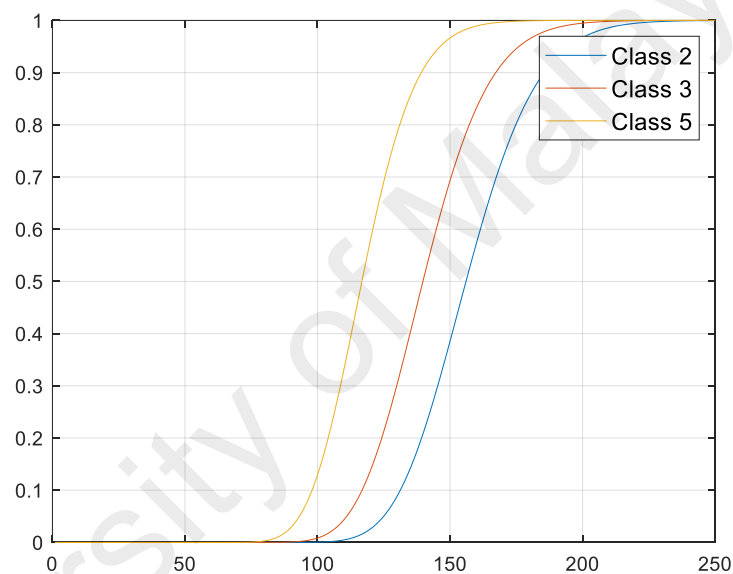


Figure 3.2: Fragility curves in reference to NESC pole class 2, 3, and 5, as simulated by MATLAB.

To conclude this segment, the poles of the 33-bus radial distribution system will be put to test in 3 different scenarios, with each, a different set of pole class parameters deployed. Each having its own unique fragility curve, every pole class will produce different failure probabilities when put to test against the same set of randomly generated windspeeds. The generation of random windspeeds will be discussed in the next segment.

3.3 Power Flow and Radial Power Flow

As introduced in the earlier segments, a 33-bus radial distribution system will be deployed to demonstrate the proposed methodology and will be modelled by using MATLAB. The power flow data is adopted from an earlier study and the single line diagram of the 33-bus distribution system is as shown in Figure 3.3 (Baran & Wu, 1989).

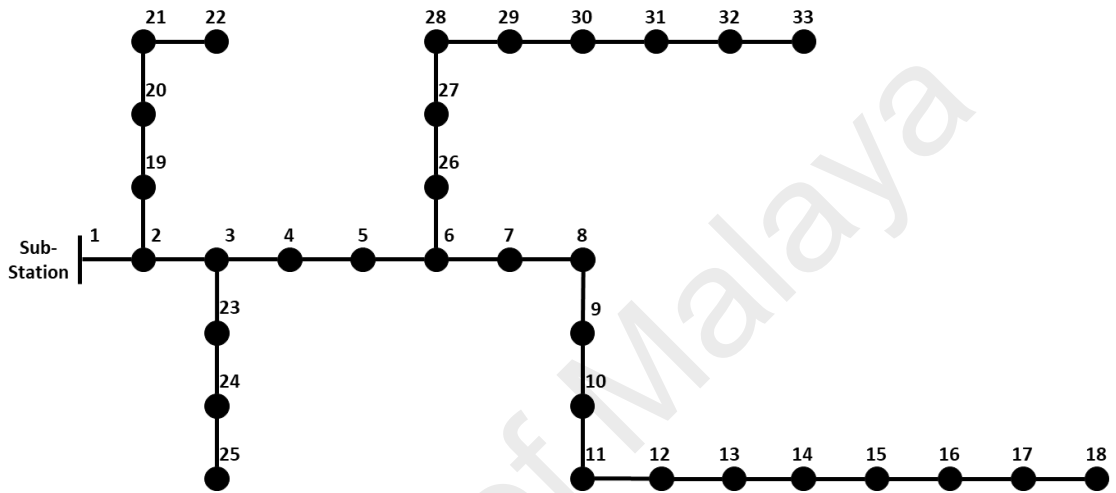


Figure 3.3: An IEEE 33-bus radial distribution system.

A power flow analysis will be executed on the 33-bus radial distribution system to obtain the steady-state value. A past study expressed the Newton-Raphson method as an analytical method designed for mesh-structured systems with many redundancies in between the generation point and load points, while backward-forward sweep methods are most effective for the purpose of analysing the power flow of radial distribution systems (Michline Rupa & Ganesh, 2014). This notion is supported by another study, stating that backward-forward sweep methodologies are often utilized to analyse radial distribution systems as these methods are observed to be computationally efficient and accurate (Chang, Chu, & Wang, 2007). This view is extended by a recent study, stating that transmission grid power flow analyses such as the Newton-Raphson, Gauss-Seidel, and fast-decoupled methods which adopt Jacobian matrix-based methodologies, typically require significant computational time and therefore is inappropriate for the application

of radial distribution systems (Ouali & Cherkaoui, 2020). Hence in this study, the backward-forward sweep method was utilized to carry out the power flow analysis on the 33-bus distribution system. As all modelling and simulation will be carried using MATLAB, the following open-source MATLAB-language M-files were adopted to simulate the necessary conditions and load flow analysis (Zimmerman & Murillo-Sanchez, 2019). The MATLAB coding as shown in Appendix A, and Appendix B.

Table 3.4: MATLAB M-Files from MATPOWER.

M-File	Purpose
case33bw.m	1) Power flow data of a 33-bus radial distribution system 2) Data adopted from earlier study (Baran & Wu, 1989)
runpf.m	1) Executes a power flow (Newton Raphson method by default) 2) Execute backward-forward method with the following command: >> runpf('case33bw', mpooption('pf.alg', 'PQSUM'))

Once the “runpf.m” function is executed in MATLAB, the power flow analysis will be carried out to generate the 33-bus radial distribution system steady-state value, which will then be utilized as the base data in this study. The base data obtained is as indicated in Appendix C.

3.4 Modelling a Stochastic Hurricane Storm

High-impact, low-probability events such as extreme weather events are typically stochastic by nature and hurricane storms are no exception. Thus, to model the influence of a hurricane storm, the “Monte-Carlo” approach is adapted in this study for the purpose of generating random windspeeds in a stochastic manner.

As expressed, natural disasters typically behave randomly. In this study, the pole fragility of the 33-bus radial distribution system will be tested against the 3-second gust speeds from the 5 different categories in the Saffir-Simpson hurricane scale.

Realistically, it is very unlikely for each pole to be subjected to the same 3-second gust speed or hurricane category for the entirety of a hurricane storm, as hurricanes typically pick up or lose speed as they move across land. Therefore, the hurricane category imposed on each pole will be generated randomly, and in addition to this, as each hurricane category has its own range of 3-second gust speeds, the latter will also be generated randomly. In short, to replicate the stochastic behaviour of a hurricane storm, each pole will be assigned a random hurricane category, before being assigned to a random 3-second gust speed from the assigned random hurricane category.

As highlighted earlier, in an actual hurricane storm, it is unlikely for each individual pole to experience constant windspeeds throughout the entire event. To mimic the conditions of an actual hurricane storm, iterations are introduced into the simulation to randomly generate a 3-second gust speed for every iteration.

Hurricane storms typically last from 12 to 24 hours, moving across land within this duration (Moloney, 2017). In this study, the entire duration of the hurricane storm is disregarded, instead, an assumption is made whereby the hurricane storm takes 10 minutes to move across each pole in the 33-bus radial distribution system. Therefore, resulting the entire duration of the event to be 330 minutes, or 5 hours and 30 minutes.

By taking into consideration that for every iteration, a 3-second gust speed is randomly generated, and 10 minutes is taken by the hurricane storm to move across each pole, 200 iterations will be required. The rationale is as shown in the following.

Time taken for hurricane to move across system = 330 minutes

Time taken for hurricane to move across each pole = 10 minutes

1 minute = 60 seconds

Therefore,

Time taken for hurricane to move across each pole = 600 seconds

1 iteration = 3 seconds (a random 3 – second gust speed is generated)

$$600 \text{ seconds} = \left(\frac{600}{3}\right) \text{ iterations}$$

$$600 \text{ seconds} = 200 \text{ iterations}$$

With every iteration, a different and random gust speed is generated, resulting in a different failure probability for each pole, and the failure probability of the current iteration will be summed up with the sum of all previous failure probabilities until the 200th and final iteration. The sum of failure probabilities for all 200 iterations will then be divided by the number of iterations to obtain the average failure probability. This will be conducted on all 33 utility poles of the distribution system, for each NESC pole class. To achieve the above, the 33-bus radial distribution system and number of iterations are firstly defined in MATLAB as shown in Figure 3.4.

```
10 - No_Of_Poles=33; %% Define No. of poles in the system
11
12 - Matrix_Class_2=zeros(3,No_Of_Poles); %% Define 3-By-33 Matrix for NESC pole class 2
13 - Matrix_Class_3=zeros(3,No_Of_Poles); %% Define 3-By-33 Matrix for NESC pole class 3
14 - Matrix_Class_5=zeros(3,No_Of_Poles); %% Define 3-By-33 Matrix for NESC pole class 5
15
16 - Monte_Carlo_Iteration=200; %% Define ite. for 5 1/2 hr hurricane storm (10 mins per pole)
```

Figure 3.4: Defining the number of poles and iterations in MATLAB.

As shown in Figure 3.4, a 3-by-33 matrix with zero values is defined for each NESC pole class. The 33 columns represent the 33 utility poles of the system while the 3 rows represent the following.

- i. Row 1 : Utility pole number of each pole (from 1 to 33)

- ii. Row 2 : Randomly generated hurricane category of each pole
- iii. Row 3 : NESC pole class of each pole

The MATLAB coding of the 3-by-33 matrix is as shown in Figure 3.5.

```

18 -   rng('shuffle');
19 -   Matrix_Class_2(1,:)=1:1:No_Of_Poles; %% Pole number from 1-to-33
20 -   Matrix_Class_2(2,:)=randi([1,5],1,No_Of_Poles); %% Random hurricane category
21 -   Matrix_Class_2(3,:)=2; % NESC pole class 2
22
23 -   Matrix_Class_3(1,:)=1:1:No_Of_Poles; %% No. of poles in the system as defined
24 -   Matrix_Class_3(2,:)=Matrix_Class_2(2,:); %% Repeat hurricane category of NESC pole class
25 -   Matrix_Class_3(3,:)=3; % NESC pole class 3
26
27 -   Matrix_Class_5(1,:)=1:1:No_Of_Poles; %% No. of poles in the system as defined
28 -   Matrix_Class_5(2,:)=Matrix_Class_2(2,:); %% Repeat hurricane category of NESC pole class
29 -   Matrix_Class_5(3,:)=5; % NESC pole class 5

```

Figure 3.5: Defining the matrix of each NESC pole class in MATLAB.

As shown in Figure 3.5, to randomly generate the hurricane categories from 1 to 5, MATLAB's "randi" function is used, as shown in the below.

randi([1,5], 1, No_Of_Poles)

Whereby in the case of this study,

[1,5] = random number to be generated from 1 to 5

1 = number of rows

No_Of_Poles = number of columns (number of poles)

The above, generates a 1-by-33 matrix containing random numbers ranging from 1 to 5 which represents the hurricane categories, as shown in the Figure 3.6.

```

Matrix_Class_2 =

Columns 1 through 23

    1     2     3     4     5     6     7     8     9    10    11    12    13    14    15    16    17    18    19    20    21    22    23
    3     2     4     3     5     4     4     4     3     1     5     4     2     2     2     3     1     3     4     1     2     3     5
    0     0     0     0     0     0     0     0     0     0     0     0     0     0     0     0     0     0     0     0     0     0     0

Columns 24 through 33

    24    25    26    27    28    29    30    31    32    33
    4     3     2     3     4     2     5     3     5     2
    0     0     0     0     0     0     0     0     0     0

Hurricane_Category =

Columns 1 through 23

    3     2     4     3     5     4     4     4     3     1     5     4     2     2     2     3     1     3     4     1     2     3     5

Columns 24 through 33

    4     3     2     3     4     2     5     3     5     2

```

Figure 3.6: Generation of random hurricane categories for each pole.

Next, MATLAB’s “for” function is used to execute a group of “if” statements, for a recurrence of 200 closed-loop iterations to replicate the 10 minutes taken for a hurricane storm to move across each pole in the 33-bus radial distribution system as indicated earlier in this segment. Then, “if” statements are deployed to check the hurricane categories generated in the 1-by-33 matrix. When the “if” statement is met, MATLAB’s “randi” function is once again utilized to generate a random number from the range of gust speeds based on each hurricane category as shown in Figure 3.7.

```

41 - for j=1:Monte_Carlo_Iteration %% for-loop will run for 200 iterations
42 -     rng('shuffle');
43 -     for i=1:length(Matrix_Class_2)
44 -         rng('shuffle');
45 -         Hurricane_Category=Matrix_Class_2(2,i);
46 -         if Hurricane_Category==1
47 -             Random_Gust_Speed=randi([93,119],1,1);
48 -         elseif Hurricane_Category==2
49 -             Random_Gust_Speed=randi([120,138],1,1);
50 -         elseif Hurricane_Category==3
51 -             Random_Gust_Speed=randi([139,162],1,1);
52 -         elseif Hurricane_Category==4
53 -             Random_Gust_Speed=randi([163,195],1,1);
54 -         elseif Hurricane_Category==5
55 -             Random_Gust_Speed=randi([196,250],1,1);
56 -         end

```

Figure 3.7: Generating random 3-second gust speeds based on the randomly generated hurricane categories in MATLAB.

Table 3.5 as shown in the below, represents the logic in which each of the “if” statements written in the “for” loop are purported to execute in accordance to.

Table 3.5: Logic used to generate random gust speed based on hurricane category.

Logical Statement	3-second gust speed (MPH)	
	IF, hurricane category is 1, generate a random gust speed from:	93
IF, hurricane category is 2, generate a random gust speed from:	120	138
IF, hurricane category is 3, generate a random gust speed from:	139	162
IF, hurricane category is 4, generate a random gust speed from:	163	195
IF, hurricane category is 5, generate a random gust speed from:	196	250

For every iteration, a failure probability is generated for each NESC pole class using the previously introduced “logncdf” function, and every failure probability generated is summed up with all previously generated failure probabilities for each NESC pole class. Once after running 200 iterations, the total sum of failure probability acquired will then be divided by the number of iterations, to obtain an averaged value of failure probability for each NESC pole class. The MATLAB coding is as shown in Figure 3.8.

```

58 -         Class_2_Mu=5.05;
59 -         Class_2_Sigma=0.135;
60 -         Pole_Failure_2(i)=logncdf(Random_Gust_Speed,Class_2_Mu,Class_2_Sigma);
61
62 -         Class_3_Mu=4.94;
63 -         Class_3_Sigma=0.140;
64 -         Pole_Failure_3(i)=logncdf(Random_Gust_Speed,Class_3_Mu,Class_3_Sigma);
65
66 -         Class_5_Mu=4.76;
67 -         Class_5_Sigma=0.137;
68 -         Pole_Failure_5(i)=logncdf(Random_Gust_Speed,Class_5_Mu,Class_5_Sigma);
69 -     end
70
71 -     Final_Pole_Failure_2=Final_Pole_Failure_2+Pole_Failure_2;
72 -     Final_Pole_Failure_3=Final_Pole_Failure_3+Pole_Failure_3;
73 -     Final_Pole_Failure_5=Final_Pole_Failure_5+Pole_Failure_5;
74 - end
75
76 - Class_2_Failure_Probability=Final_Pole_Failure_2/j
77 - Class_3_Failure_Probability=Final_Pole_Failure_3/j
78 - Class_5_Failure_Probability=Final_Pole_Failure_5/j

```

Figure 3.8: Generating failure probability for each NESC pole class.

The modelling of the hurricane storm and the generation of the failure probability are summarized and shown in Figure 3.9.

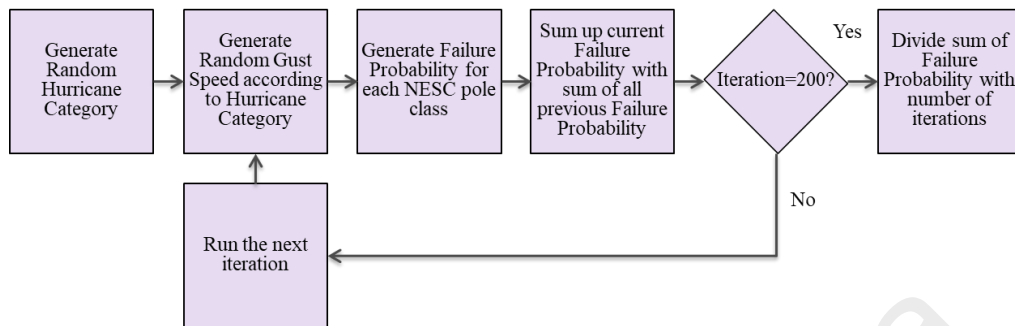


Figure 3.9: Process flow in generating failure probabilities with respect to the randomly generated hurricane gust speeds.

Since the failure probability values are decimal numbers that fall within the range of 0 to 1, a threshold value is assumed to determine the failure of the poles. As this research is scientific based, it is preferable to adopt a principle rather than to make a baseless assumption of a threshold value. Therefore, in this study, Pareto's 80/20 principle is adopted. Pareto's 80/20 principle suggests that in various events, approximately 80% of the consequences are a product of 20% of the causes (Dunford, Su, Tamang, & Wintour, 2014). This can be applied to the failure probability in this study whereby, any failure probability value generated within the range of the top 20% represents failure. Since the value of "1" represents definite failure, top 20% of the value of "1" would mean any value generated at 0.8 and above. Thus, based on Pareto's 80/20 principle, the failure threshold point can be set at 0.8.

Upon identifying which of the poles in the 33-bus distribution system has failed, this information will then be superimposed on to the steady-state value of each bus obtained from the backward-forward power flow analysis introduced in the previous segment, thus replicating power loss and interruption due to a hurricane storm event. The written MATLAB coding is as shown in Appendix D.

3.5 Timeline of Hurricane Storm Event

For the purpose of this study, the timeline of the event is assumed as shown in Figure 3.10.

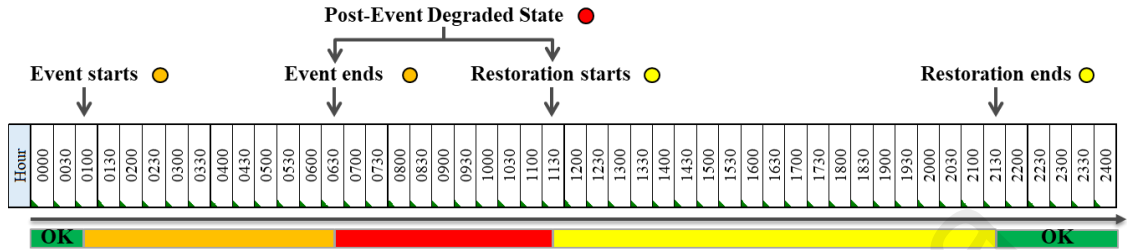


Figure 3.10: Timeline of hurricane storm event.

3.6 Process Flow Chart

In this study, the flow of the works carried out is as shown in Figure 3.11.

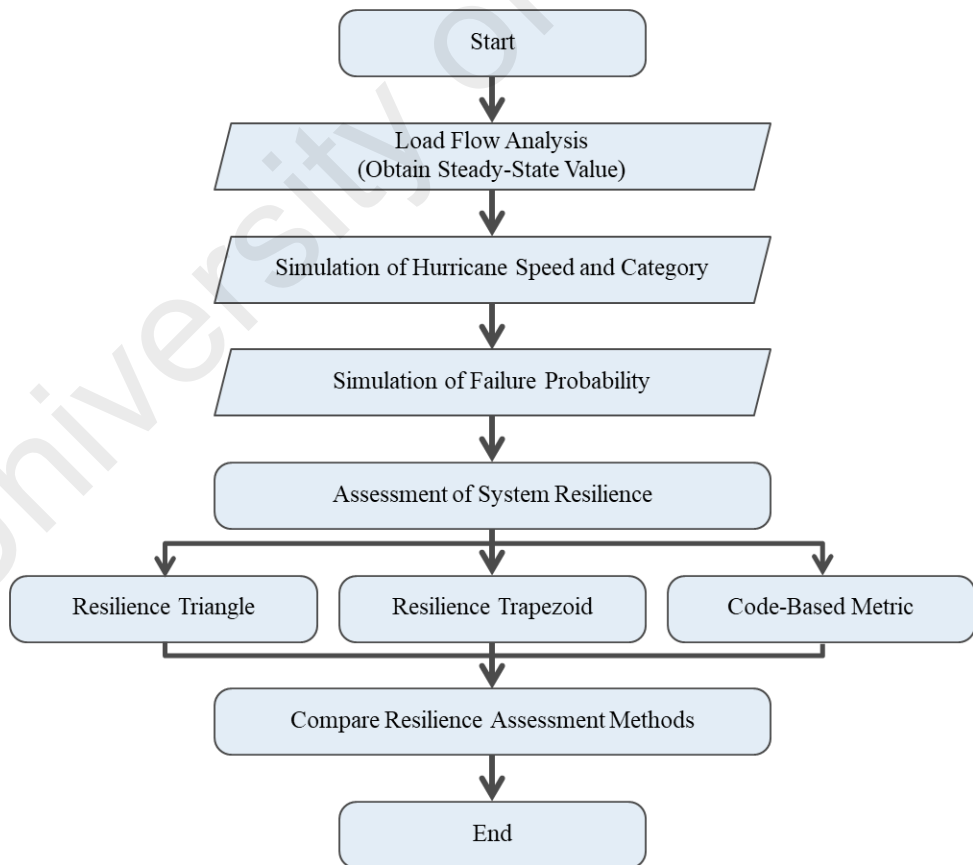


Figure 3.11: Flow chart of the evaluation of resilience assessment methods

3.7 Resilience Assessment

Thus far, the earlier segments have indicated that the execution of this study involves quantitative methodologies with the 2 key factors below.

- i. Assessing resilience by means of fragility modelling
- ii. Assessing impact assessment with a probabilistic approach

To expand on the above to key factors, it has been expressed in the earlier segments, that the base of the study involves subjecting the distribution poles of a 33-bus distribution system to a hurricane storm before evaluating its resilience. As indicated in the previous segment, this study will deploy 3 pole classes in accordance to the NESC standards, and the impact of the simulated hurricane storm will differ for each pole class due to each having a different fragility curve. Therefore, in order to achieve one of the many research objectives of completing the resilience assessment of the 33-bus distribution system, individual evaluation will be carried out on each of the following.

- i. Resilience of distribution system with NESC Class 2 poles
- ii. Resilience of distribution system with NESC Class 3 poles
- iii. Resilience of distribution system with NESC Class 5 poles

While the primary assessment method proposed is the resilience trapezoid approach, to fulfil the objective of this research, other quantitative assessment methods used to quantify resilience should also be considered. Discussions will be carried out in this segment on the three proposed resilience assessment methods in the below.

- i. Resilience Triangle
- ii. Resilience Trapezoid
- iii. Code-Based Resilience Metrics

3.7.1 Resilience Triangle

The “Resilience Triangle” was first introduced in a past publication, for the purpose of plotting the functionality levels of an infrastructure system post event and the duration required for the system to restore to its pre-event state (Tierney & Bruneau, 2007). The generic resilience triangle can be represented with Figure 3.12.

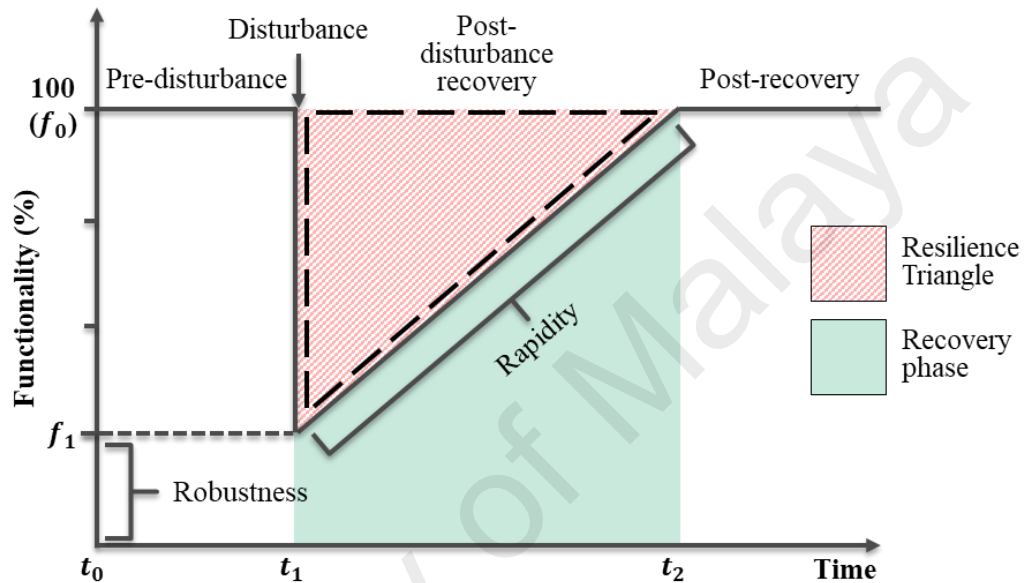


Figure 3.12: A generic resilience triangle.

Once the resilience triangle is mapped, mitigation strategies can then be formed to improve the robustness of the infrastructure system to minimize functionality loss due to disruptive events, in other words, reducing the decline in the vertical axis. Additionally, enhancement strategies should be defined to decrease the restoration time which is represented by the horizontal axis. Since the parameters of both the vertical axis and horizontal axis will directly impact the area of the resilience triangle, the resilience triangle can then be utilized to reflect the resilience of the infrastructure system. However, the area of the resilience triangle should not be the only metric used to indicate the performance of an infrastructure system.

Ultimately, by plotting the parameters to map the resilience triangle, the metrics as shown in Table 3.6, can be obtained and utilized to quantify resilience.

Table 3.6: The resilience triangle metrics.

Resilience Metric	Description
Resilience Loss	Degradation of functionality and performance due to the occurrence of a disruptive event (Hosseini, Baker, & Ramirez-Marquez, 2016).
	While it is represented by the area of the resilience triangle, other parameters should be considered as two resilience triangles might have the same area despite having different proportions in the loss of functionality and restoration time (Zobel, 2010).
Robustness	Capacity of the infrastructure system to tolerate a certain degree of stress or tension, without being subjected to functionality loss and thus can be represented by the available functionality upon a disruptive event (Cimellaro, Reinhorn, & Bruneau, 2010).
Recovery	Time taken to restore the infrastructure system's degraded functionality levels post-event, to functionality levels at pre-event.
	It should be noted that the restoration period generally includes mobilization time by the service or recovery team to the site of damage, and the lead time for certain replacement parts for damaged components.
Rapidity	Rate of recovery post-event, during the restoration period (Cimellaro, Reinhorn, & Bruneau, 2010).

By referring to Figure 3.12, the mathematical representation of the metrics above can be expressed as shown in Table 3.7.

Table 3.7: Mathematical expression of the resilience triangle metrics.

Resilience Metric	Mathematical Expression
Resilience Loss	$\frac{(t_2 - t_1) \times (f_0 - f_1)}{2} \quad (3.3)$
Robustness	$f_1 \quad (3.4)$
Recovery	$t_2 - t_1 \quad (3.5)$
Rapidity	$\frac{(f_0 - f_1)}{(t_2 - t_1)} \quad (3.6)$

In this study, the resilience triangle metrics will be utilized to measure the resilience of the 33-bus distribution system in the following two areas.

- i. Operational functionality – load connected in kilowatts
- ii. Infrastructural functionality – number of distribution poles

Once the MATLAB simulation of the hurricane storm and the pole failure probabilities of the 33-bus distribution system are ran, the total disconnected load and failed poles can be obtained, thus allowing the robustness of the system to be measured via the decline in functionality. Next, the recovery of the system will be measured with an assumed restoration time of 10 hours. Similarly, the rapidity of the system can also be measured with the assumed restoration time, with the addition of the functionality recovered. Finally, the area of the resilience triangle is measured with the functionality loss and assumed restoration time, to obtain the loss of resilience.

3.7.2 Resilience Trapezoid

The resilience trapezoid was proposed in an earlier study, as an expansion to the resilience triangle (Panteli, Trakas, Mancarella, & Hatziargyriou, 2017). As discussed in the previous chapter, the resilience trapezoid has multiple phases, thereby enabling an effective evaluation through the breaking down of each phase. Hence, this provides an extension to the capabilities of the resilience triangle method which is only able to execute single-phase evaluations. Additionally, unlike the resilience triangle which assumes an instantaneous drop in functionality upon a disruptive event, the resilience trapezoid takes on an approach with a gradual functionality degradation. As shown in the next page, Figure 3.13 depicts the resilience trapezoid, along with the metrics used to measure the parameters of each phase.

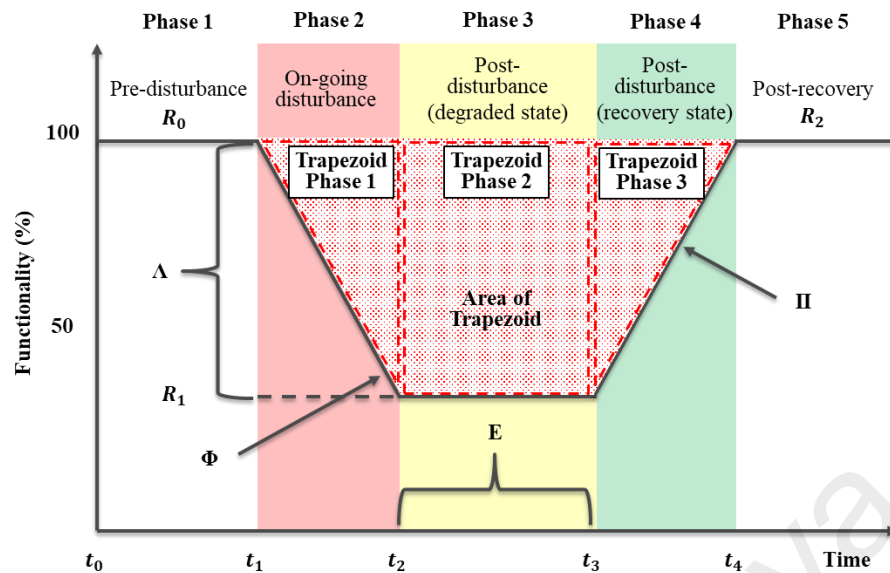


Figure 3.13: The $\Phi\Lambda E\Pi$ metrics of the resilience trapezoid.

As introduced in the previous chapter, the “ $\Phi\Lambda E\Pi$ ” metrics which are specific to each phase, can be utilized to quantify the resilience of an infrastructure of a system. Similar to the proposed approach in the previous segment, the resilience trapezoid assessment method will also be utilized to evaluate the resilience of the 33-bus distribution system from the perspective of its operational and infrastructural functionality. The same values of total disconnected load and failed poles simulated in MATLAB used in the resilience triangle method would be used as the base data used of the resilience trapezoid.

From Figure 3.13, it is observed that there are several differences between the resilience triangle and resilience trapezoid. Unlike the resilience triangle, the resilience trapezoid takes into consideration, the gradual decline in functionality levels rather than an instantaneous drop. Thus, upon the MATLAB simulation of the hurricane storm and the pole failure probabilities of the 33-bus distribution system, the resilience trapezoid’s “ Φ ” metric can be obtained by measuring the gradient of the decline in functionality levels over the duration of the hurricane storm, whereby in the case of this study is 5.5 hours. Additionally, unlike the resilience triangle which measures the remaining functionality

after an event as the robustness of the infrastructure system, the “ Λ ” metric of the resilience trapezoid is measured as the functionality loss instead.

Another difference between the resilience triangle and the resilience trapezoid is that the latter takes into account, the response time required before any restoration work can begin and thus, the infrastructure system can be assumed as being under a “degraded” state. Measured as the “E” metric, and in the case of this study, the post-event degraded state is assumed to be 5 hours.

Next, similar to the resilience triangle’s rapidity metric, the “ Π ” metric of the resilience trapezoid is measured as the recovery rate of the infrastructure system’s functionality and can be obtained by measuring the gradient of the increment in functionality levels over the recovery time required. Here, following the same approach used in the resilience triangle assessment, the recovery time is assumed to be 10 hours. An additional point to highlight; the unlike the resilience triangle, the resilience trapezoid does not consider the recovery time as a specific metric. By referring to Figure 3.13, the mathematical representation of the resilience trapezoid’s metrics can be expressed as shown in Table 3.8.

Table 3.8: The $\Phi\Lambda E\Pi$ metrics of the resilience trapezoid.

Metric	Description	Mathematical Expression
Φ	Rate of functionality decline (how steep is gradient)	$\frac{(R_1 - R_0)}{(t_2 - t_1)} \quad (3.7)$
Λ	Decline in functionality level	$R_0 - R_1 \quad (3.8)$
E	Duration of post-disturbance degraded state (how long before restoration can begin)	$t_3 - t_2 \quad (3.9)$
Π	Rate of functionality recovery (how steep is gradient)	$\frac{(R_2 - R_1)}{(t_4 - t_3)} \quad (3.10)$

Supplementing the $\Phi\Lambda E\Pi$ metrics, is the area of the resilience trapezoid as indicated in Figure 3.13. Similar to the resilience triangle, the resilience trapezoid represents resilience loss. However, while the resilience triangle reflects only one phase, the resilience triangle can be broken down into 3 phases with each phase having its own individual area. It should also be noted that just as the resilience triangle is dependent on its metrics – robustness and recovery, the resilience trapezoid is dependent on its $\Phi\Lambda E\Pi$ metrics. Finally, to obtain the total area of the resilience trapezoid, the areas of all 3 phases are summed up. The areas of each of the resilience trapezoid’s phase can be mathematically expressed as shown in Table 3.9.

Table 3.9: Mathematical expressions of each phase within the resilience trapezoid.

Trapezoid Phase	Shape	Mathematical Expression
1	Triangle (most left)	$\frac{(R_0 - R_1) \times (t_2 - t_1)}{2}$ (3.11)
2	Rectangle	$(R_0 - R_1) \times (t_3 - t_2)$ (3.12)
3	Triangle (most right)	$\frac{(R_2 - R_1) \times (t_4 - t_3)}{2}$ (3.13)

3.7.3 Code-Based Resilience Metrics

Adopted from an earlier study, the “Code-Based Resilience Metrics” is the third and final resilience method to be carried out for the purpose of evaluating the operational and infrastructural resilience of the 33-bus distribution system. While it is dependent on the functionality levels and the duration of the disruptive event, the code-based method measures the resilience required, whereas the resilience triangle and resilience trapezoid methods measure resilience loss. Most of the code-based resilience metrics are derived from specific empirical equations. The primary metric, however, is represented by variables that are assigned based on the duration of the event, in orders of 10. These

variables are as shown in Figure 3.14 (Chanda, Srivastava, Mohanpurkar, & Hovsapian, 2018).

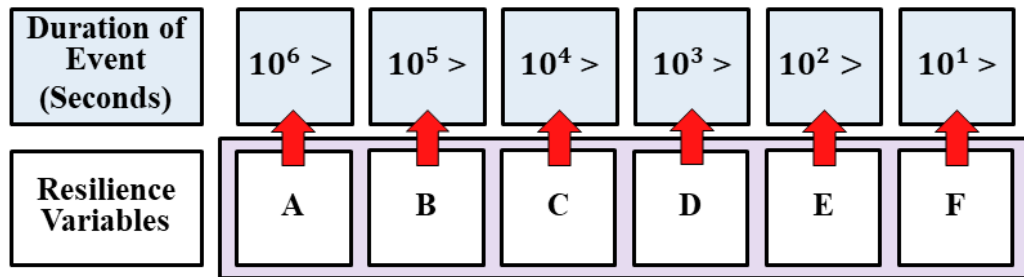


Figure 3.14: Resilience variable with corresponding event duration in orders of 10.

Next, the functionality levels are measured but unlike the resilience triangle and the resilience trapezoid, the code-based method considers on the fraction of functionality unaffected by disruption. Below, is the mathematical representation of this metric.

$$f = \frac{\text{functionality unaffected by disruptive event}}{\text{total functionality of infrastructure system}} \quad (3.14)$$

Whereby,

$$f = \text{fraction of functionality}$$

An additional feature of the code-based method is the segregation of resilience levels into three categories as shown in Table 3.10 (Chanda, Srivastava, Mohanpurkar, & Hovsapian, 2018).

Table 3.10: The code-based resilience metrics resilience categories.

R	1	2	3	4	5	6	7	8	9
	Low Resilience			Moderate Resilience			High Resilience		
R*	1.00- 3.71	3.72- 6.42	6.43- 9.13	9.14- 11.85	11.86- 14.56	14.57- 17.27	17.28- 19.98	19.99- 22.70	22.71- 25.41

In reference to Table 3.10, the “R*” value can be calculated by using the equation below, and once the “R*” value is obtained, the resilience category, “R” can be determined.

$$R^* = (\alpha + e^f)(1 + f) \quad (3.15)$$

Whereby,

α = duration of disruptive event in seconds, without the order of ten

f = fraction of functionality

University of Malaya

CHAPTER 4: RESULTS AND DISCUSSIONS

4.1 Introduction

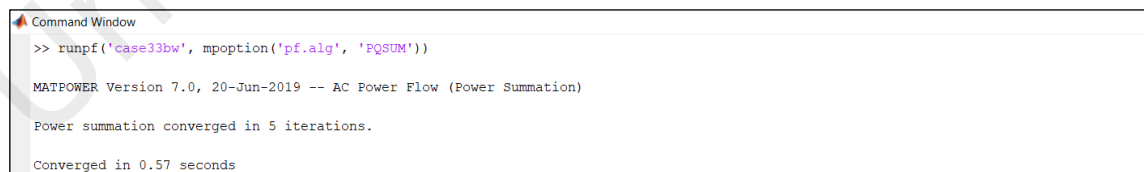
In this chapter, discussions will be carried out on the various resilience assessment methods introduced in the earlier chapters. As stated in the methodology chapter, resilience assessment frameworks will be deployed to evaluate the post-event state of a 33-bus distribution system. Each of the resilience assessment method will be used to assess the scenarios with 3 different NESC pole class ratings. Comparisons will be drawn and summarized based on the merits and disadvantages of each assessment method.

4.2 Results from MATLAB Simulation

In this segment, the outputs from the MATLAB simulated failure probabilities will be further discussed.

4.2.1 Base Value: 33-Bus Distribution System's Steady State

To obtain the base data values of this research, a power flow analysis of the 33-bus radial distribution was carried out by executing the “runpf.m” M-file in MATLAB with the “case33bw.m” M-file as the input. The simulation was executed in MATLAB's command window, as shown in Figure 4.1.



```
Command Window
>> runpf('case33bw', mpooption('pf.alg', 'PQSUM'))

MATPOWER Version 7.0, 20-Jun-2019 -- AC Power Flow (Power Summation)

Power summation converged in 5 iterations.

Converged in 0.57 seconds
```

Figure 4.1: Execution of “runpf.m” in MATLAB's command window.

While the simulation resulted in the steady-state power flow values of the 33-bus distribution system's buses and branches, the focal point and necessary information,

however, lies specifically in the load consumption of the buses. Table 4.1 is the compiled power flow data of the buses.

Table 4.1: Power flow data of the 33-bus radial distribution system

Bus	Voltage		Generation		Load	
No.	Magnitude (pu)	Phase (deg)	P (MW)	Q (MVA _r)	P (MW)	Q (MVA _r)
1	1.000	0.000	3.92	2.44	0.00	0.00
2	0.997	0.014	0.00	0.00	0.10	0.06
3	0.983	0.096	0.00	0.00	0.09	0.04
4	0.975	0.162	0.00	0.00	0.12	0.08
5	0.968	0.228	0.00	0.00	0.06	0.03
6	0.950	0.134	0.00	0.00	0.06	0.02
7	0.946	-0.096	0.00	0.00	0.20	0.10
8	0.941	-0.060	0.00	0.00	0.20	0.10
9	0.935	-0.133	0.00	0.00	0.06	0.02
10	0.929	-0.196	0.00	0.00	0.06	0.02
11	0.928	-0.189	0.00	0.00	0.04	0.03
12	0.927	-0.177	0.00	0.00	0.06	0.04
13	0.921	-0.269	0.00	0.00	0.06	0.04
14	0.919	-0.347	0.00	0.00	0.12	0.08
15	0.917	-0.385	0.00	0.00	0.06	0.01
16	0.916	-0.408	0.00	0.00	0.06	0.02
17	0.914	-0.485	0.00	0.00	0.06	0.02
18	0.913	-0.495	0.00	0.00	0.09	0.04
19	0.997	0.004	0.00	0.00	0.09	0.04
20	0.993	-0.063	0.00	0.00	0.09	0.04
21	0.992	-0.083	0.00	0.00	0.09	0.04
22	0.992	-0.103	0.00	0.00	0.09	0.04
23	0.979	0.065	0.00	0.00	0.09	0.05
24	0.973	-0.024	0.00	0.00	0.42	0.20
25	0.969	-0.067	0.00	0.00	0.42	0.20
26	0.948	0.173	0.00	0.00	0.06	0.03
27	0.945	0.229	0.00	0.00	0.06	0.03
28	0.934	0.312	0.00	0.00	0.06	0.02
29	0.926	0.390	0.00	0.00	0.12	0.07
30	0.922	0.496	0.00	0.00	0.20	0.60
31	0.918	0.411	0.00	0.00	0.15	0.07
32	0.917	0.388	0.00	0.00	0.21	0.10
33	0.917	0.380	0.00	0.00	0.06	0.04
		Total	3.92	2.44	3.71	2.32

As indicated in Table 4.1, bus 1 is recognized at the generator or PV bus., and the two columns on the right indicates the load consumption of each bus, which totals up to 3.71 MW. Buses 24 and 25 have the highest load consumption at 0.42 MW each, while bus 11 has the lowest consumption at 0.04 MW. To note, in this study, it is not necessary to consider the reactive power.

4.2.2 Simulation of Hurricane Storm and Pole Failure

The earlier chapter established that a hurricane storm of 5 categories of windspeeds would be simulated with MATLAB, followed by the modelling of 3 fragility curves based on 3 NESC pole class characteristics, in which would determine the failure probabilities of the 33-bus radial distribution system. As suggested in the previous chapter, the threshold value which dictates the pole failure would be any value at 0.8 and above. In this study, the MATLAB coding as shown in Appendix D, was executed and results are as compiled in Table 4.2. Additionally, the MATLAB command window output is as attached in Appendix E.

Table 4.2: MATLAB simulated hurricane category and pole failure probability

Hurricane Category	Class 2		Class 3		Class 5	
	Failure Probability	Pole Number	Failure Probability	Pole Number	Failure Probability	Pole Number
1	0.0044	1	0.0343	1	0.2496	1
2	0.0900	2	0.2924	2	0.7556	2
1	0.0050	3	0.0374	3	0.2586	3
1	0.0052	4	0.0039	4	0.2707	4
2	0.0913	5	0.2966	5	0.7625	5
1	0.0048	6	0.0367	6	0.2594	6
2	0.0880	7	0.2899	7	0.7559	7
2	0.0867	8	0.2856	8	0.7502	8
3	0.4078	9	0.6993	9	0.9626	9
3	0.3812	10	0.6748	10	0.9563	10
2	0.0885	11	0.2909	11	0.7569	11
3	0.4018	12	0.6927	12	0.9605	12
2	0.0865	13	0.2847	13	0.7480	13

2	0.0889	14	0.2911	14	0.7563	14
5	0.9895	15	0.9985	15	1.0000	15
2	0.0914	16	0.2965	16	0.7611	16
5	0.9909	17	0.9987	17	1.0000	17
3	0.3869	18	0.6795	18	0.9575	18
1	0.0043	19	0.0329	19	0.2378	19
3	0.3865	20	0.6820	20	0.9591	20
1	0.0050	21	0.0372	21	0.2580	21
4	0.8257	22	0.9497	22	0.9982	22
5	0.9917	23	0.9988	23	1.0000	23
1	0.0050	24	0.0372	24	0.2572	24
1	0.0047	25	0.0351	25	0.2488	25
2	0.0874	26	0.2883	26	0.7542	26
3	0.4036	27	0.6942	27	0.9609	27
3	0.4208	28	0.7102	28	0.9649	28
1	0.0047	29	0.0361	29	0.2582	29
3	0.4001	30	0.6903	30	0.9595	30
2	0.0855	31	0.2828	31	0.7467	31
5	0.9902	32	0.9986	32	1.0000	32
5	0.9913	33	0.9988	33	1.0000	33

Table 4.2 as shown in the above, points out the randomly generated hurricane category for each of the 33-bus radial distribution poles. Three sets of failure probabilities were generated, with differing values, due to the different parameters of each NESC pole class. The status of each pole as represented under the “Pole Number” column, is differentiated in accordance to the colour in which each cell is highlighted with. While the simulated failure probabilities between the NESC pole classes are non-identical, the cases of Class 2 and Class 3 does have the same poles that failed and subsequently went offline. Table 4.3 indicates the pole status of each pole in accordance to the colour highlighted.

Table 4.3: Indication of pole status

Indicator	Pole Status	Remarks
GREEN	Online	Did not succumb to failure due to hurricane
RED	Failed	Pole broken and offline due to hurricane
GREY	Offline	Pole not broken, but offline due to prior broken/offline pole

As stated in the earlier chapter, the resilience of the 33-bus distribution system will be assessed in the areas of the operational and infrastructural functionality of the system. To following segments will attempt to carry out further discussions on both areas based on the results obtained from the MATLAB simulations.

4.2.3 Operational Functionality

To obtain the operational functionality at a more generic level, the total disconnected load is measured. As this 33-bus distribution system is a radial network, the failure of any pole will lead to every other subsequent pole connected to it to go offline. In the case of this study, failed poles are poles broken as a result of succumbing to the hurricane intensity. On the other hand, the offline poles are poles that suffered disruption due to a prior broken or offline pole but remain infrastructurally unaffected by the hurricane intensity. Therefore, the total disconnected load must include the loads of both the failed and offline poles. Table 4.4 is a compilation of the load losses due to pole breakdown and pole offline, for each NESC pole class.

Table 4.4: Total disconnected load (MW) of each NESC pole class.

Class 2		Class 3		Class 5	
Pole Number	Load (MW)	Pole Number	Load (MW)	Pole Number	Load (MW)
1	0.00	1	0.00	1	0.00
2	0.10	2	0.10	2	0.10
3	0.09	3	0.09	3	0.09
4	0.12	4	0.12	4	0.12
5	0.06	5	0.06	5	0.06
6	0.06	6	0.06	6	0.06
7	0.20	7	0.20	7	0.20
8	0.20	8	0.20	8	0.20
9	0.06	9	0.06	9	0.06
10	0.06	10	0.06	10	0.06
11	0.04	11	0.04	11	0.04
12	0.06	12	0.06	12	0.06
13	0.06	13	0.06	13	0.06

14	0.12	14	0.12	14	0.12
15	0.06	15	0.06	15	0.06
16	0.06	16	0.06	16	0.06
17	0.06	17	0.06	17	0.06
18	0.09	18	0.09	18	0.09
19	0.09	19	0.09	19	0.09
20	0.09	20	0.09	20	0.09
21	0.09	21	0.09	21	0.09
22	0.09	22	0.09	22	0.09
23	0.09	23	0.09	23	0.09
24	0.42	24	0.42	24	0.42
25	0.42	25	0.42	25	0.42
26	0.06	26	0.06	26	0.06
27	0.06	27	0.06	27	0.06
28	0.06	28	0.06	28	0.06
29	0.12	29	0.12	29	0.12
30	0.20	30	0.20	30	0.20
31	0.15	31	0.15	31	0.15
32	0.21	32	0.21	32	0.21
33	0.06	33	0.06	33	0.06
Total Disconnected Load	1.56	Total Disconnected Load	1.56	Total Disconnected Load	2.73

Finally, a simple approach of calculating the ratio of the total disconnected load against the total load prior to the hurricane storm, will indicate the operational functionality levels of the system via the total connected loads, as shown in Table 4.5.

Table 4.5: Generic measurement of the 33-bus distribution system’s operational functionality levels.

NESC Pole Class		2	3	5
Total Load	(MW)	3.71	3.71	3.71
Total Disconnected Load	(MW)	1.56	1.56	2.73
	(%)	42%	42%	74%
Total Connected Load	(MW)	2.15	2.15	0.98
	(%)	58%	58%	26%

4.2.4 Infrastructural Functionality

The infrastructural functionality of the 33-bus distribution system is assessed differently in comparison to the approach taken to assess operational functionality. In the assessment of the operational functionality, the points of interest include the failed poles and the offline poles. To obtain infrastructural functionality at a generic level, only the number of poles which are infrastructurally intact is necessary, and the loads connected to every pole of the system is neglected regardless of the condition on the poles the loads are connected to respectively. Conversely, the number of poles broken due to the hurricane intensity may also be considered.

In this study, however, only the broken poles of the 33-bus distribution system will be examined to obtain the infrastructural functionality, and the review will be carried out for poles from the 3 NESC pole classes. Table 4.6 is a compilation of the broken poles, which are indicated with red colour-filled cells, for each NESC pole class.

Table 4.6: Total broken poles of each NESC pole class

Class 2		Class 3		Class 5	
Pole Number	Infrastructural Status	Pole Number	Infrastructural Status	Pole Number	Infrastructural Status
1	Intact	1	Intact	1	Intact
2	Intact	2	Intact	2	Intact
3	Intact	3	Intact	3	Intact
4	Intact	4	Intact	4	Intact
5	Intact	5	Intact	5	Intact
6	Intact	6	Intact	6	Intact
7	Intact	7	Intact	7	Intact
8	Intact	8	Intact	8	Intact
9	Intact	9	Intact	9	Broken
10	Intact	10	Intact	10	Broken
11	Intact	11	Intact	11	Intact
12	Intact	12	Intact	12	Broken
13	Intact	13	Intact	13	Intact
14	Intact	14	Intact	14	Intact
15	Broken	15	Broken	15	Broken

16	Intact	16	Intact	16	Intact
17	Broken	17	Broken	17	Broken
18	Intact	18	Intact	18	Broken
19	Intact	19	Intact	19	Intact
20	Intact	20	Intact	20	Broken
21	Intact	21	Intact	21	Intact
22	Broken	22	Broken	22	Broken
23	Broken	23	Broken	23	Broken
24	Intact	24	Intact	24	Intact
25	Intact	25	Intact	25	Intact
26	Intact	26	Intact	26	Intact
27	Intact	27	Intact	27	Broken
28	Intact	28	Intact	28	Broken
29	Intact	29	Intact	29	Intact
30	Intact	30	Intact	30	Broken
31	Intact	31	Intact	31	Intact
32	Broken	32	Broken	32	Broken
33	Broken	33	Broken	33	Broken
Total Broken Poles	6	Total Broken Poles	6	Total Broken Poles	14

Finally, a simple approach of calculating the ratio of the total broken poles against the total number of poles, will indicate the infrastructural functionality levels of the system, as shown in the table below, as shown in Table 4.7.

Table 4.7: Generic measurement of the 33-bus distribution system's infrastructural functionality levels

NESC Pole Class		2	3	5
Total Number of Poles	(No.)	33	33	33
Total Broken Poles	(No.)	6	6	14
	(%)	18%	18%	42%
Total Poles Intact	(No.)	27	27	19
	(%)	82%	82%	58%

4.3 Evaluating the 33-Bus Distribution System with the Resilience Triangle Metrics

In this segment, the data from the MATLAB simulated outputs will be further examined by deploying the resilience triangle assessment method. Since the simulated failure probabilities for NESC pole class 2 and 3 scenarios are the same, the assessment will of both will be carried out at the same time.

4.3.1 Operational Functionality and Resilience

By plotting the load data of NESC pole class 2, 3, and 5 during the entire timeline of the event, the following graphs are obtained and are as shown in Figures 4.2, 4.3, and 4.4.

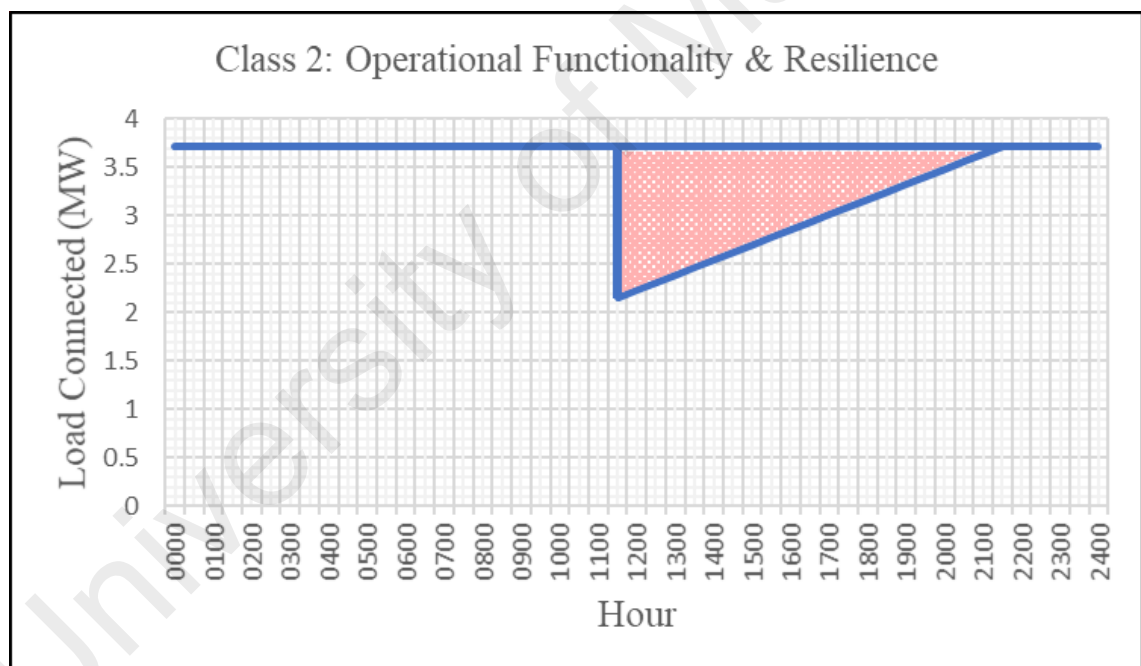


Figure 4.2: 33-bus distribution system's operational functionality and resilience with NESC pole class 2 ratings.

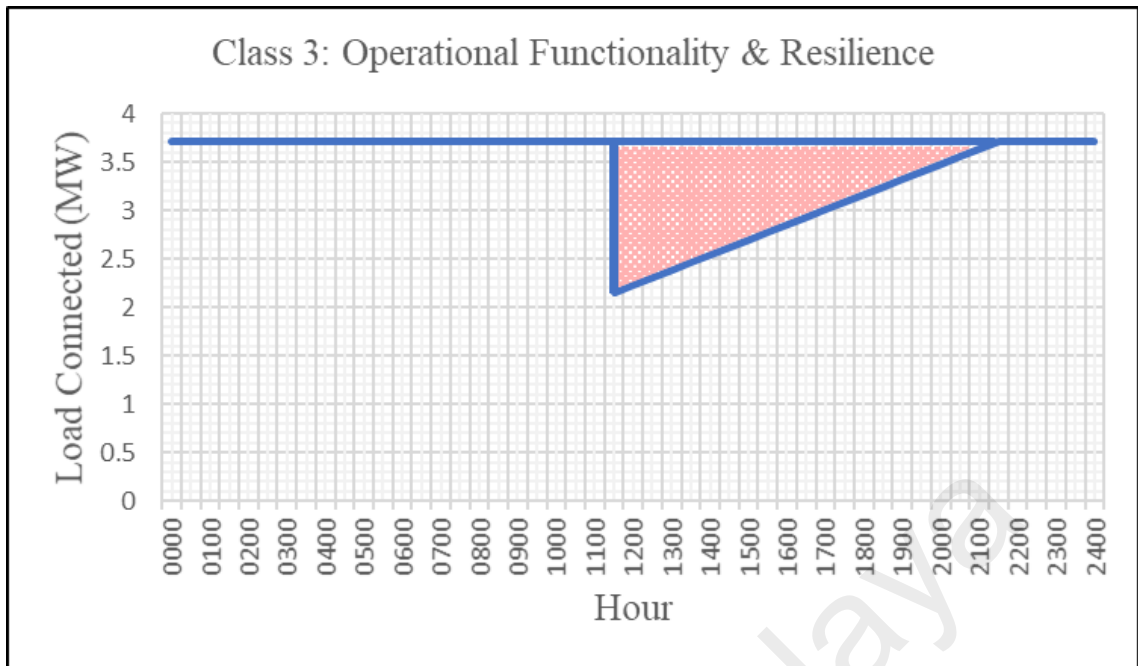


Figure 4.3: 33-bus distribution system's operational functionality and resilience with NESC pole class 3 ratings.

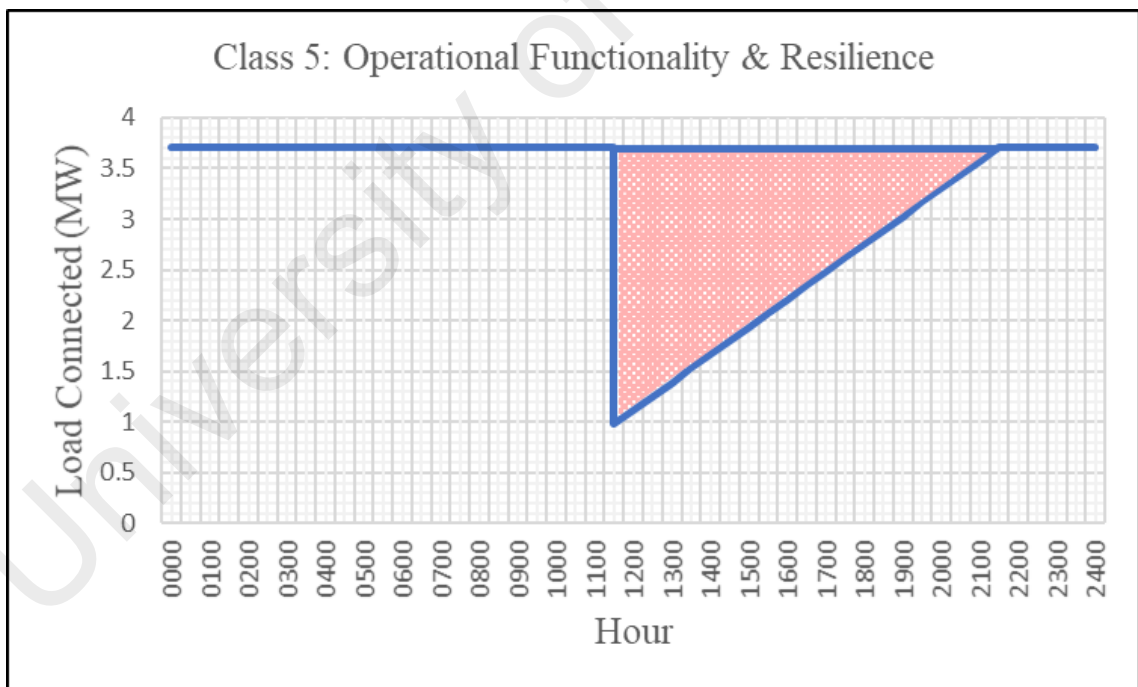


Figure 4.4: 33-bus distribution system's operational functionality and resilience with NESC pole class 5 ratings.

By extracting the information from each of the graphs shown, the metrics as shown in Table 4.8, are obtained using the mathematical expressions introduced in the earlier chapter, to represent the operational functionality and resilience of the 33-bus distribution system.

Table 4.8: Operational resilience triangle metrics of the 33-bus distribution system for NESC pole class 2, 3, and 5.

Metric	NESC Poles Class 2	NESC Poles Class 2	NESC Poles Class 5
Resilience Loss	7.8 MW-Hour	7.8 MW-Hour	13.65 MW-Hour
Loss of Functionality	1.56 MW	1.56 MW	2.73 MW
Robustness	2.15 MW	2.15 MW	0.98 MW
Recovery	10 Hour	10 Hour	10 Hour
Rapidity	0.16 MW/Hour	0.16 MW/Hour	0.27 MW/Hour

From Table 4.8, it can be summarized that the loss of functionality is most significant in the scenario whereby the 33-bus distribution system is fitted with NESC class 5 poles. Additionally, the loss of functionality signifies lower levels of robustness as indicated in the table above. As a result, the resilience loss suffered by the NESC class 5 scenario is also the significantly higher when compared to the other NESC pole class scenarios which have higher levels of robustness and lower levels of functionality loss. However, since the recovery metric, which is the denominator for the rapidity metric, is assumed to be 10 hours for all 3 NESC pole classes, the NESC pole class 5 scenario has the highest rapidity, due to it having loss the highest levels of functionality amongst the 3 scenarios. Therefore, by assuming that all 3 scenarios recover to pre-event functionality levels in the same duration of 10 hours, the scenario with the highest loss of functionality will have the highest rate of recovery.

Lastly, focusing on the most crucial metric of all metrics – the resilience loss, it is observed that NESC pole class 5 scenario suffered approximately 175% of the operational resilience losses sustained by the NESC pole classes 2, and 3.

4.3.2 Infrastructural Functionality and Resilience

Similarly, by plotting the pole failure data of NESC pole class 2, 3, and 5 during the entire timeline of the event, the following graphs are obtained and are as shown in Figures 4.5, 4.6, and 4.7.

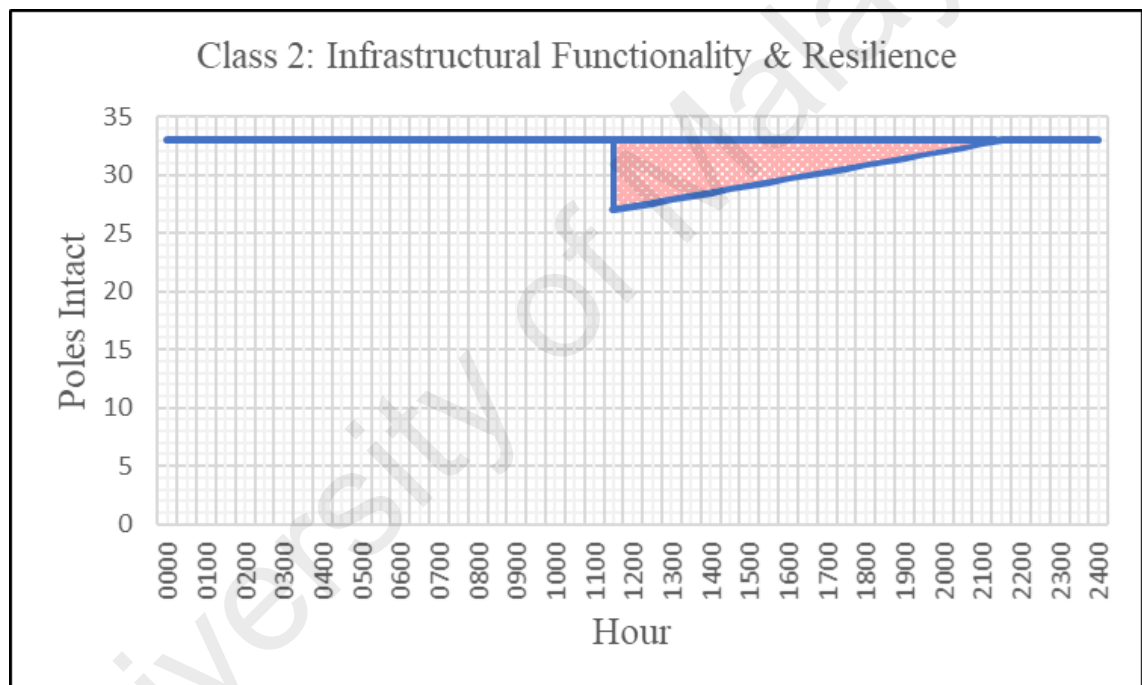


Figure 4.5: 33-bus distribution system’s infrastructural functionality and resilience with NESC pole class 2 ratings.

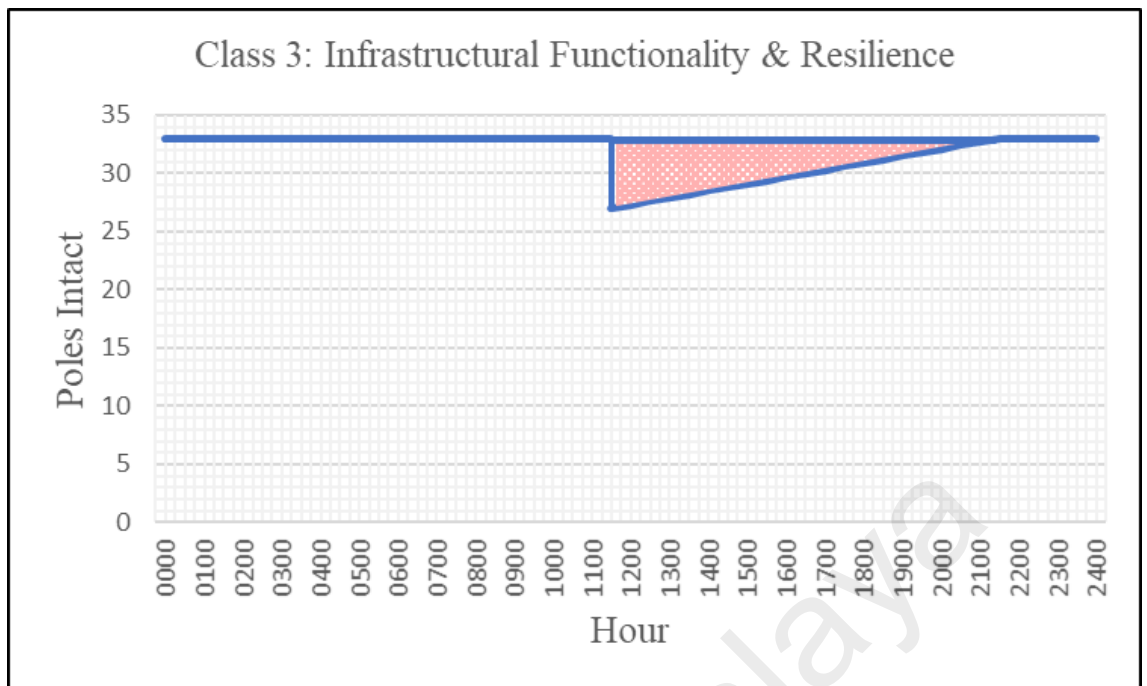


Figure 4.6: 33-bus distribution system's infrastructural functionality and resilience with NESC pole class 3 ratings.

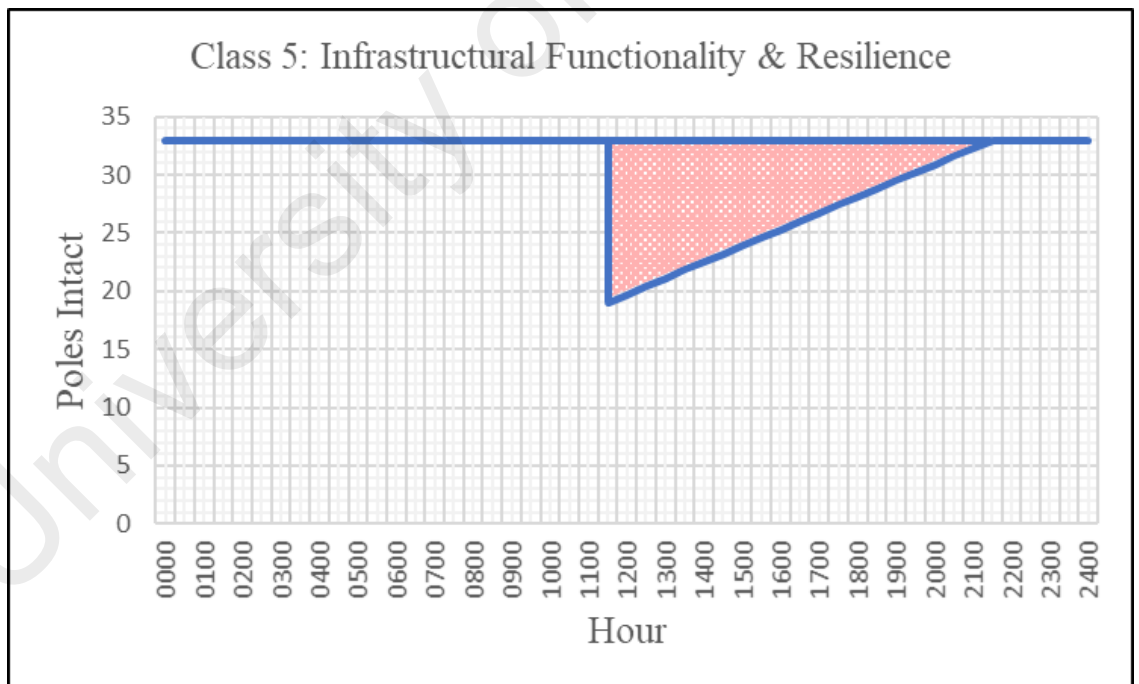


Figure 4.7: 33-bus distribution system's infrastructural functionality and resilience with NESC pole class 5 ratings.

By extracting the information from each of the graphs shown, the metrics as shown in Table 4.9, are obtained using the mathematical expressions introduced in the earlier chapter, to represent the infrastructural functionality and resilience of the 33-bus distribution system.

Table 4.9: Infrastructural resilience triangle metrics of the 33-bus distribution system for NESC pole class 2, 3, and 5.

Metric	NESC Poles Class 2	NESC Poles Class 2	NESC Poles Class 5
Resilience Loss	30 Pole-hour	30 Pole-hour	70 Pole-hour
Loss of Functionality	6 Pole	6 Pole	14 Pole
Robustness	27 Pole	27 Pole	19 Pole
Recovery	10 Hours	10 Hours	10 Hours
Rapidity	0.6 Pole/Hour	0.6 Pole/Hour	1.4 Pole/Hour

From Table 4.9, it can be summarized that in the scenario whereby the 33-bus distribution system is fitted with NESC class 5 poles, the loss of infrastructural functionality is most notable. Also, the loss of functionality indicates lower levels of robustness as shown in the table above. As a result, the NESC class 5 scenario reflects the highest resilience loss in comparison to the other NESC pole class scenarios which have higher levels of robustness and lower losses in functionality. Again, resembling the assessment in the earlier segment, as the recovery metric is assumed to be 10 hours for all 3 NESC pole classes, the NESC pole class 5 scenario has the highest rapidity, due to it having the highest levels of infrastructural functionality loss amongst the 3 scenarios. Thus, by assuming that all 3 scenarios recover to pre-event functionality levels in the same duration of 10 hours, the scenario with the highest loss of infrastructural functionality will have the highest rate of recovery.

When focused on the resilience loss, it is observed that NESC pole class 5 scenario suffered approximately 233% of the infrastructural resilience losses sustained by the NESC pole classes 2, and 3.

4.4 Evaluating the 33-Bus Distribution System with the Resilience Trapezoid Metrics

In this segment, the data from the MATLAB simulated outputs will be further examined by utilizing the resilience trapezoid assessment method. Similar to the earlier segment, as the simulated failure probabilities for NESC pole class 2 and 3 scenarios are the same, the assessment will of both will be carried out at the same time.

4.4.1 Operational Functionality and Resilience

By plotting the load data of NESC pole class 2, 3, and 5 of the entire event timeline, the following graphs are obtained and are as shown in Figures 4.8, 4.9, and 4.10.

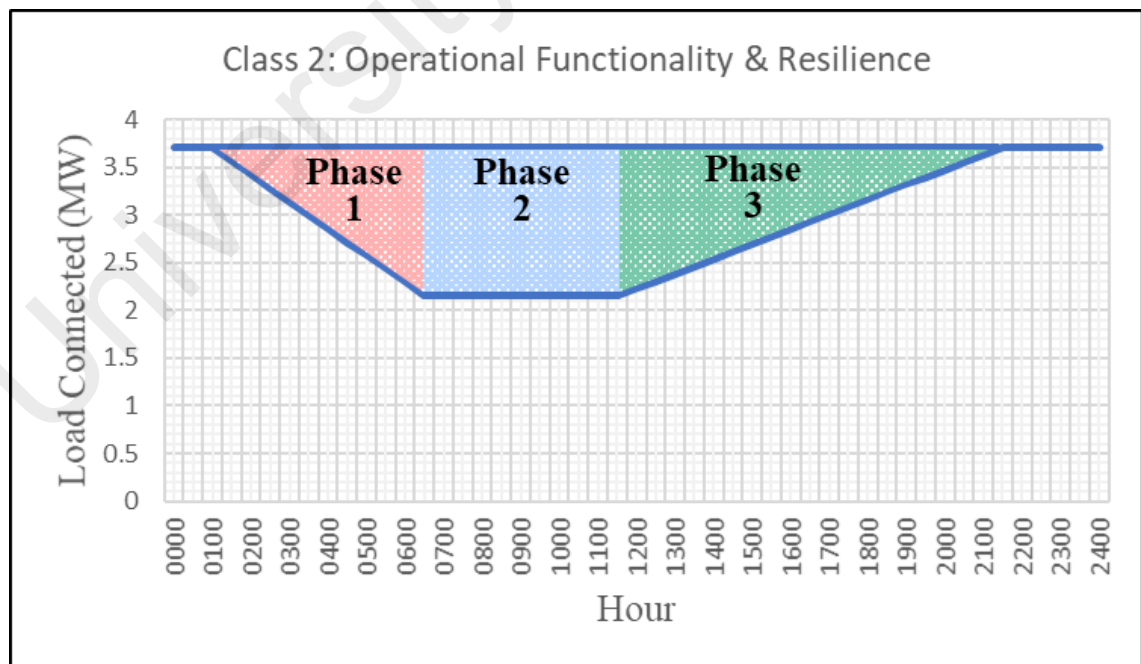


Figure 4.8: 33-bus distribution system's operational functionality and resilience with NESC pole class 2 ratings.

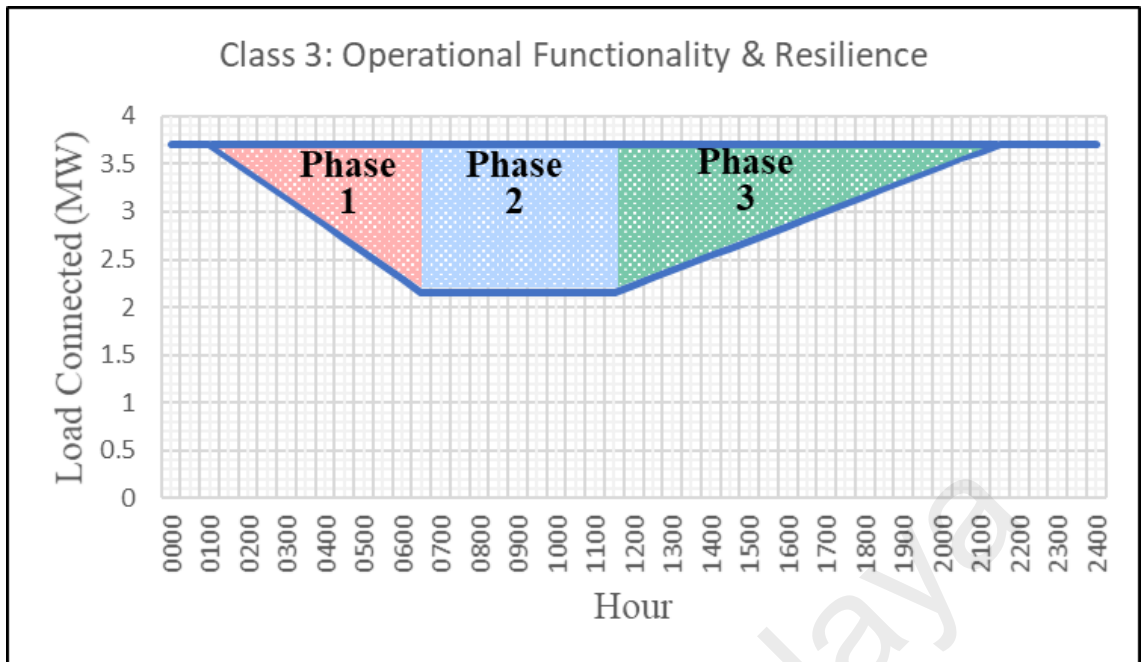


Figure 4.9: 33-bus distribution system’s operational functionality and resilience with NESC pole class 3 ratings.

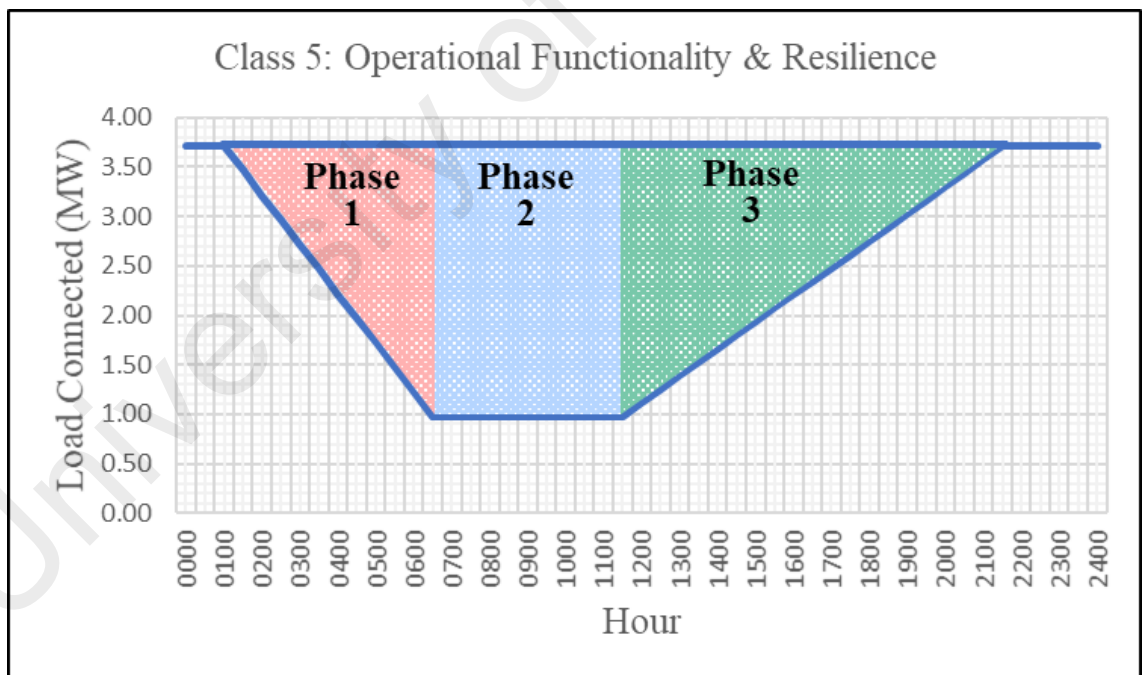


Figure 4.10: 33-bus distribution system’s operational functionality and resilience with NESC pole class 5 ratings.

By extracting the information from each of the graphs shown, the metrics as shown in Table 4.10, are obtained using the mathematical expressions introduced in the earlier chapter, to represent the operational functionality and resilience of the 33-bus distribution system.

Table 4.10: The operational $\Phi\Lambda E\Pi$ resilience trapezoid metrics of the 33-bus distribution system for NESC pole class 2, 3, and 5.

Metric	NESC Pole Class 2	NESC Pole Class 3	NESC Pole Class 5
Φ	-0.28 MW/Hour	-0.28 MW/Hour	-0.50 MW/Hour
Λ	1.56 MW	1.56 MW	2.73 MW
E	5 Hours	5 Hours	5 Hours
Π	0.16 MW/Hour	0.16 MW/Hour	0.27 MW/Hour

In addition to the metrics above, to assess the resilience loss, the area of the trapezoid is broken down into 3 phases as shown in Table 4.11.

Table 4.11: The operational resilience loss of the 33-bus distribution system for NESC pole class 2, 3, and 5

Trapezoid Phase	NESC Pole Class 2	NESC Pole Class 3	NESC Pole Class 5
1 (Left Triangle)	4.29 MW-Hour	4.29 MW-Hour	7.51 MW-Hour
2 (Center Rectangle)	7.80 MW-Hour	7.80 MW-Hour	13.65 MW-Hour
3 (Right Triangle)	7.80 MW-Hour	7.80 MW-Hour	13.65 MW-Hour
Total Trapezoid Area	19.89 MW-Hour	19.89 MW-Hour	34.81 MW-Hour

From Tables 4.10 and 4.11, it can be summarized that the NESC pole class 5 scenario has the highest loss of operational functionality at 2.73 MW in comparison to NESC pole class 2 and 3, with each losing 1.56 MW in operational functionality. This also indicates

that the NESC pole class 5 scenario has the most rapid decline in operational functionality when struck by the hurricane storm, declining at 0.50 MW per hour, while NESC pole class 2 and 3 each have declining rates of 0.28 MW per hour. However, since the recovery time is assumed to be 10 hours for all 3 NESC pole classes, the NESC pole class 5 scenario is able to achieve the highest rate of recovery, due to it having loss the highest levels of functionality amongst the 3 scenarios.

Lastly, by examining the trapezoid areas of all 3 NESC pole classes, it can be concluded that the NESC pole class 5 scenario has the highest resilience loss at 34.81 MW-Hour, in comparison to NESC pole classes 2 and 3, each at 19.89 MW-Hour. However, upon further inspection of the 3 trapezoid phases, it is observed that the restoration stage in trapezoid phase 3, contributed to 39% of the total resilience loss, in addition to another 39% resilience loss contributed by the system's degraded state in trapezoid phase 2. The high percentage of resilience loss in trapezoid phase 3 is likely due to the recovery duration at 10 hours, which is approximately 182% of the event duration of 5.5 hours. This is confirmed as the resilience loss in trapezoid phase 3 is approximately 182% of the resilience loss suffered by the system in trapezoid phase 1. Thus, by reducing the amount of time in which the system is in a degraded state and by improving response time along with resources to shorten restoration time, the resilience loss suffered by the system can be reduced, regardless of whichever NESC pole class scenario.

4.4.2 Infrastructural Functionality and Resilience

Similarly, by plotting the pole failure data of NESC pole class 2, 3, and 5 during the entire timeline of the event, the following graphs are obtained and are as shown in Figures 4.11, 4.12, and 4.13.

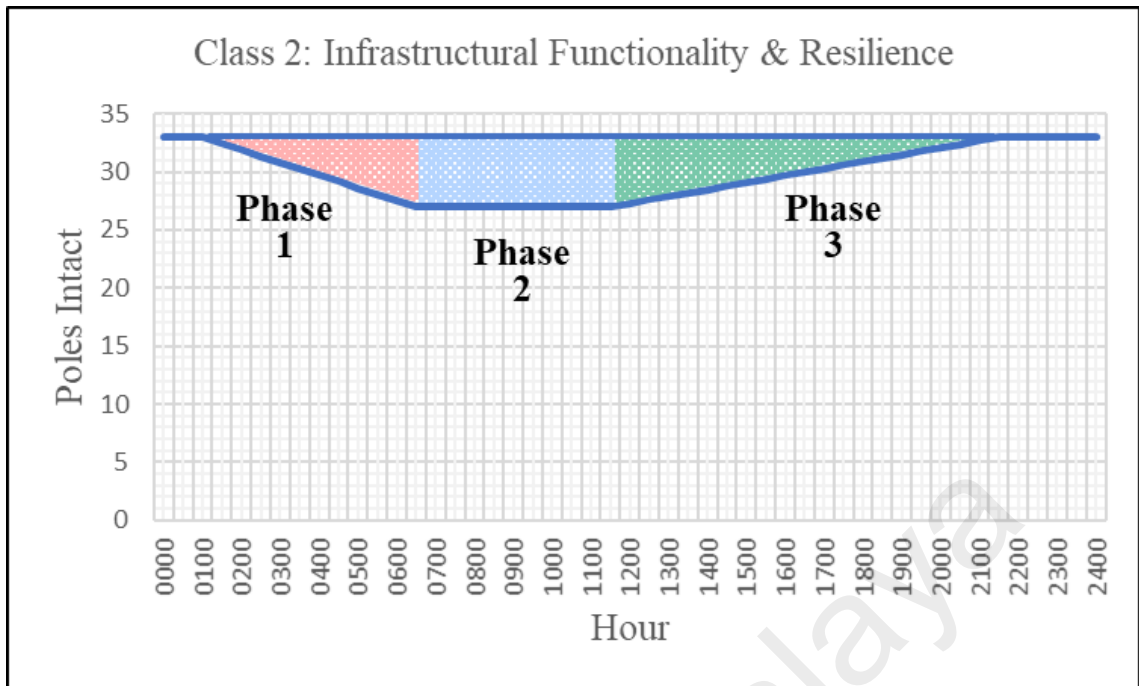


Figure 4.11: 33-bus distribution system's infrastructural functionality and resilience with NESC pole class 2 ratings.

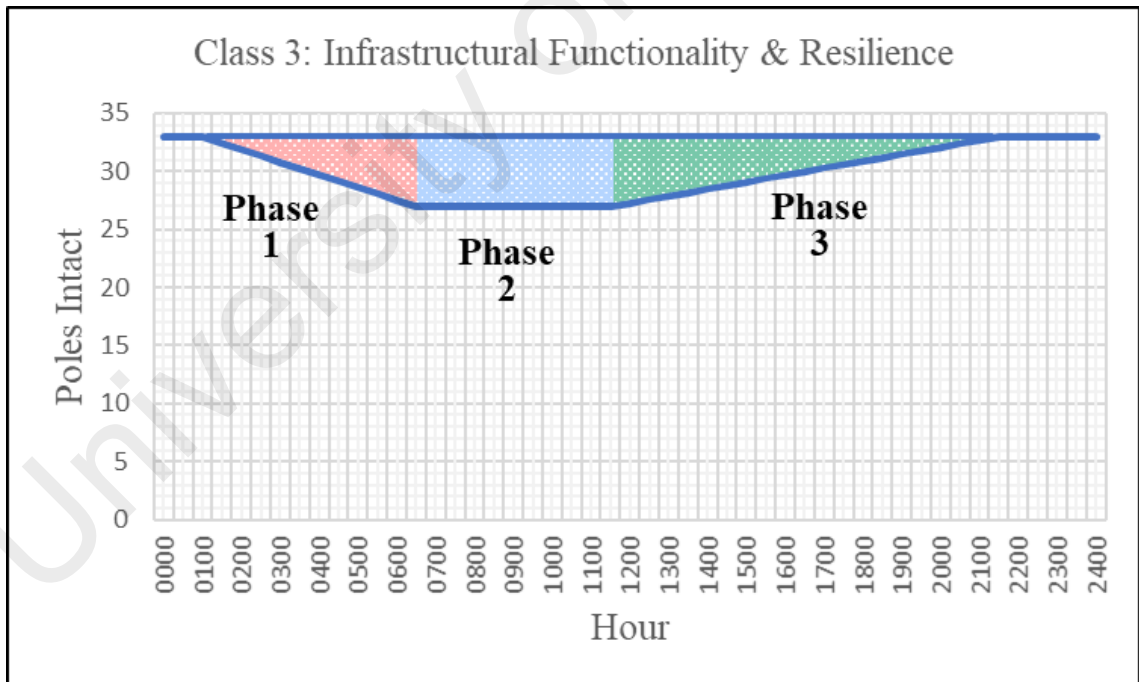


Figure 4.12: 33-bus distribution system's infrastructural functionality and resilience with NESC pole class 3 ratings.

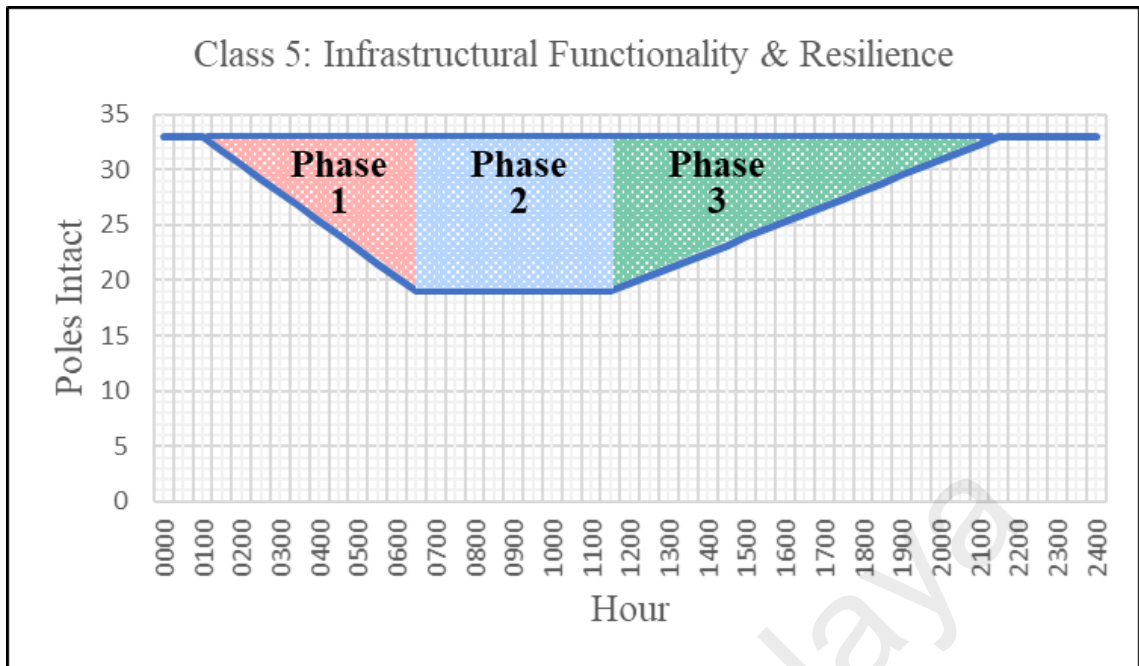


Figure 4.13: 33-bus distribution system's infrastructural functionality and resilience with NESC pole class 5 ratings.

By extracting the information from each of the graphs shown, the metrics as shown in Table 4.12, are obtained using the mathematical expressions introduced in the earlier chapter, to represent the infrastructural functionality and resilience of the 33-bus distribution system.

Table 4.12: The infrastructural $\Phi\Lambda E\Pi$ resilience trapezoid metrics of the 33-bus distribution system for NESC pole class 2, 3, and 5.

Metric	NESC Pole Class 2	NESC Pole Class 3	NESC Pole Class 5
Φ	-1.09 Pole/Hour	-1.09 Pole/Hour	- 2.55 Pole/Hour
Λ	6 Pole	6 Pole	14 Pole
E	5 Hours	5 Hours	5 Hours
Π	0.6 Pole/Hour	0.6 Pole/Hour	1.4 Pole/Hour

In addition to the metrics shown in Table 4.12, to assess the resilience loss, the area of the trapezoid is broken down into 3 phases as shown in Table 4.13.

Table 4.13: The infrastructural resilience loss of the 33-bus distribution system for NESC pole class 2, 3, and 5.

Trapezoid Phase	NESC Pole Class 2	NESC Pole Class 3	NESC Pole Class 5
1 (Left Triangle)	16.5 Pole-Hour	16.5 Pole-Hour	38.5 Pole-Hour
2 (Center Rectangle)	30.0 Pole-Hour	30.0 Pole-Hour	70.0 Pole-Hour
3 (Right Triangle)	30.0 Pole-Hour	30.0 Pole-Hour	70.0 Pole-Hour
Total Trapezoid Area	76.5 Pole-Hour	76.5 Pole-Hour	178.5 Pole-Hour

By analysing the data shown in Tables 4.12 and 4.13, NESC pole class 5 scenario is observed to suffer the highest infrastructural functionality loss at 14 poles in comparison to NESC pole class 2 and 3, with each losing 6 poles. This would also contribute to a steeper decline in infrastructural functionality for NESC pole class 5, as the hurricane storm duration is the same for all NESC pole classes. Still, as the recovery time is assumed to be 10 hours for all 3 NESC pole classes, the NESC pole class 5 scenario is able to achieve the highest rate of recovery, due to it having the highest loss in functionality amongst the 3 scenarios.

Additionally, by observing the trapezoid areas of all 3 NESC pole classes, it can be concluded that the NESC pole class 5 scenario has the highest resilience loss at 178.5 Pole-Hour, in comparison to NESC pole classes 2 and 3, each at 76.5 Pole-Hour. Nevertheless, when examined further, it is observed that the restoration stage in trapezoid phase 3, contributed to 39% of the total resilience loss, in addition to another 39% resilience loss contributed by the system's degraded state in trapezoid phase 2. This is consistent with the findings from the operational functionality assessment whereby the

cause of the resilience loss in trapezoid phase 3 can be linked to the recovery duration at 10 hours, which is approximately 182% of the event duration of 5.5 hours. This is further verified as the resilience loss in trapezoid phase 3 is approximately 182% of the resilience loss suffered by the system in trapezoid phase 1.

4.5 Evaluating the 33-Bus Distribution System with the Code-Based Resilience Metrics

In this segment, the data from the MATLAB simulated outputs will be further examined by utilizing the code-based metrics assessment method. As previously mentioned, the simulated failure probabilities for NESC pole class 2 and 3 scenarios are the same, and therefore the assessment will of both will be carried out at the same time.

4.5.1 Operational Functionality and Resilience

The variables as shown in Table 4.14, are required in the assessment of the 33-bus distribution system's operational functionality and resilience.

Table 4.14: Necessary variables for the assessment of the 33-bus distribution system's operational functionality and resilience.

Variable	NESC Pole Class 2	NESC Pole Class 3	NESC Pole Class 5
Functionality unaffected	2.15 MW	2.15 MW	0.98 MW
Total functionality	3.71 MW	3.71 MW	3.71 MW
Total duration of hurricane storm	1.98×10^4 s	1.98×10^4 s	1.98×10^4 s

With the values as presented in Table 4.14, the following metrics as shown in Table 4.15, are determined using the mathematical expressions as introduced in the earlier chapter.

Table 4.15: The code-based resilience metrics for the operational functionality and resilience of the 33-bus distribution system for NESC pole class 2, 3, and 5.

Variable	NESC Pole Class 2	NESC Pole Class 3	NESC Pole Class 5
Fraction of Functionality, f	0.58	0.58	0.26
Resilience Variable	B ($> 10^4 s$)	B ($> 10^4 s$)	B ($> 10^4 s$)
Total duration of hurricane storm	$1.98 \times 10^4 s$	$1.98 \times 10^4 s$	$1.98 \times 10^4 s$
Resilience Range Determinant, R^*	5.95	5.95	4.13
Resilience Level, R	2 (Low Resilience)	2 (Low Resilience)	2 (Low Resilience)

From the data presented in the tables, it is observed that NESC pole classes 2 and 3, each have values of fraction of functionality, f , at 0.58, which can also be represented as 58% of functionality levels. On the other hand, NESC pole class 5 has the lowest fraction of functionality, f , at 0.26, which essentially projects 26% of functionality levels. Despite the apparent difference in functionality levels at a staggering 223%, all 3 NESC pole class scenarios fall under the same resilience level, R, at “Low Resilience”. Additionally, the NESC pole class 5 scenario is distinguished as having the lowest resilience range determinant, R^* value of 4.13, while NESC pole classes 2 and 3, each have resilience range determinant, R^* values of 5.95. While the metric of resilience range determinant, R^* was primarily utilized to determine the resilience level, R, it may also be deployed to indicate the resilience levels of each scenario, which in this study points out NESC pole classes 2 and 3, as having the highest resilience, followed by NESC pole class 5.

4.5.2 Infrastructural Functionality and Resilience

The variables as shown in Table 4.16, are required in the assessment of the 33-bus distribution system's infrastructural functionality and resilience.

Table 4.16: Necessary variables for the assessment of the 33-bus distribution system's infrastructural functionality and resilience.

Variable	NESC Pole Class 2	NESC Pole Class 3	NESC Pole Class 5
Functionality unaffected	27 Poles	27 Poles	19 Poles
Total functionality	33 Poles	33 Poles	33 Poles
Total duration of hurricane storm	$1.98 \times 10^4 s$	$1.98 \times 10^4 s$	$1.98 \times 10^4 s$

With the values as presented in Table 4.16, the metrics as shown in Table 4.17, are determined using the mathematical expressions as introduced in the earlier chapter.

Table 4.17: The code-based resilience metrics for the infrastructural functionality and resilience of the 33-bus distribution system for NESC pole class 2, 3, and 5

Variable	NESC Pole Class 2	NESC Pole Class 3	NESC Pole Class 5
Fraction of Functionality, f	0.82	0.82	0.58
Resilience Variable	B ($> 10^4 s$)	B ($> 10^4 s$)	B ($> 10^4 s$)
Total duration of hurricane storm	$1.98 \times 10^4 s$	$1.98 \times 10^4 s$	$1.98 \times 10^4 s$
Resilience Range Determinant, R*	7.74	7.74	5.95
Resilience Level, R	3 (Low Resilience)	3 (Low Resilience)	2 (Low Resilience)

From the data presented in Tables 4.16 and 4.17, it is observed that NESC pole classes 2 and 3, each have values of fraction of functionality, f, at 0.82, which can also be

represented as the 33-bus distribution system having 82% of its poles intact. On the other hand, NESC pole class 5 has the lowest fraction of functionality, f , at 0.58, or rather 58%. Despite a less significant difference between the infrastructural functionality levels in comparison to the difference between the operational functionality levels, the variance is still significant at 141%. On a higher level, all 3 NESC pole class scenarios fall under the same resilience level, R , at “Low Resilience”, however, when investigated at a lower tier, the NESC pole class 5 scenario is distinguished as having the lowest resilience range determinant, R^* value of 5.95, which results in a R -value of “2”, while NESC pole classes 2 and 3, each have resilience range determinant, R^* values of 7.74, which results in a R -value of “3”. This subsequently concludes that NESC pole classes 2 and 3, have the highest resilience, followed by NESC pole class 5.

4.6 Evaluation of the Resilience Assessment Methods

In this segment, the resilience assessment methods deployed to assess the data from the MATLAB simulated outputs will be further examined and evaluated, with a final segment to summarize the merits and attributes of each method.

4.6.1 Evaluation of the Resilience Triangle Assessment Method

Observations from the earlier segment involving the resilience assessment of the 33-bus distribution system with the resilience triangle suggests that the resilience triangle’s hypotenuse is dependent on the restoration efforts and recovery rate. Ideally, the gradient of the hypotenuse should be as steep as possible, to reflect a high recovery rate. In this study, the resilience triangle’s hypotenuse is plotted as a linear line, however, in real world scenarios, many unforeseeable factors may be induced into the restoration stage. In reality, the triangle’s hypotenuse may be exponential or even triangular, subject to the

actual environment and unpredictable factors. However, to reduce the complexity of the assessment, a linear line can be mapped to estimate the recovery rate of the system.

While the resilience triangle assessment approach enables the system's functionality and resilience restoration phase to be mapped and obtained, it is however, unable to capture other critical phases undergone by the system during a disastrous event. Due to this limitation, the resilience triangle is unable to map out the degradation and degraded phase of the system. Thus, important information such as the deterioration rate of the system's functionality and resilience, and waiting time undergone by the system before restoration may take place, are disregarded, and is as shown in Figure 4.14.

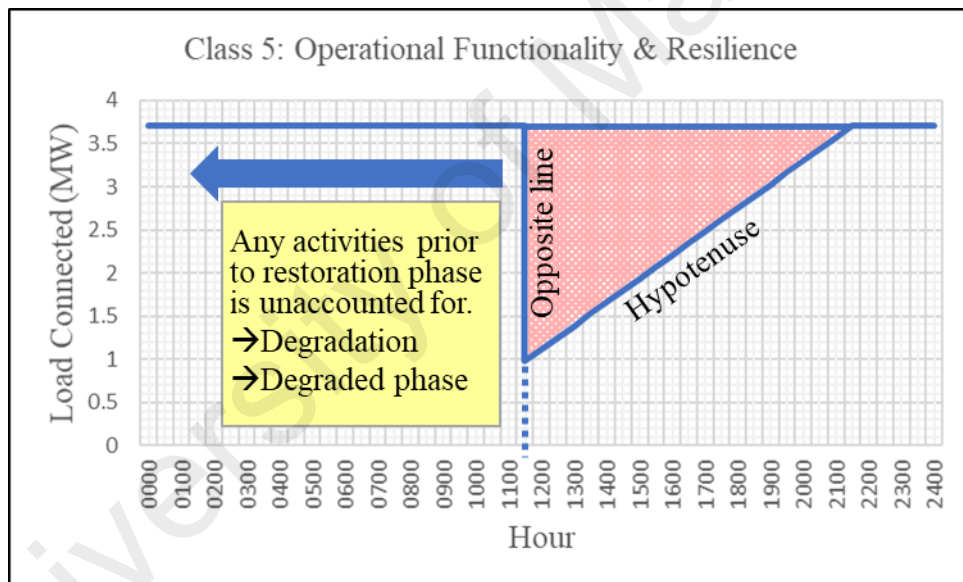


Figure 4.14: Critical information disregarded by the resilience triangle assessment method.

In the case of this study, the hurricane storm occurs from 0100 to 0630 hours, followed by a post-event phase in which the system is in a degraded state from 0630 to 1130 hours. However, as shown in Figure 4.14, the opposite-line of the resilience triangle is plotted only at the point whereby the 33-bus distribution system has completely undergone the hurricane storm and is at its lowest functionality and resilience level, before the plotting

of the hypotenuse which represents the system's recovery phase. This is perhaps the most critical limitation of the resilience triangle, as this reflects that the resilience triangle does not have the capacity to provide a complete and thorough breakdown of all the phases in which any system typically has to undergo upon being impacted by a disastrous event. Furthermore, without such key information, the resilience of a system cannot be evaluated phase-by-phase and therefore the appropriate prevention and mitigation strategies to reduce the impact of a high-impact, low-probability event cannot be planned and adapted.

To conclude, the resilience triangle may be deployed to assess single high-impact, low-probability events, at a high level. Should the ultimate concerns be the loss of functionality and resilience, and how quickly a system is restored to full functionality, the resilience triangle assessment method is a method which fits the requirement.

4.6.2 Evaluation of the Resilience Trapezoid Assessment Method

As expressed in chapter 2, past studies have suggested the resilience trapezoid as an extension of the resilience triangle. This is evident from the observations made during the earlier segment involving the resilience assessment of the 33-bus distribution system with the resilience trapezoid as the resilience trapezoid enabled the complete mapping of all the phases that the system undergone, along with the transition from one phase to another.

The 3 individual areas which total up to form the resilience trapezoid, can be used to indicate the phase of which the system is undergoing. Thus, an evaluation will be carried out for each phase as presented in the following.

i. Phase 1: Most-left Triangle in Resilience Trapezoid

With the triangle as shown in Figure 4.15, the degradation phase is plotted to represent the system's functionality and resilience which are succumbing gradually to the hurricane storm. Ideally, the gradient of the triangle's hypotenuse should be as horizontally flat as possible, to indicate a slow degradation rate.

In this study, the triangle's hypotenuse is plotted as a linear line, however, in real world scenarios, many unforeseeable factors may be induced into the degradation stage. In reality, the triangle's hypotenuse may be exponential or even triangular, subject to the actual environment and unpredictable factors. However, to reduce the complexity of the assessment, a linear line can be mapped to estimate the recovery rate of the system. With this triangle, enhancement strategies can be designed to increase to the endurance and robustness of a system so that the rate and extent of degradation can be reduced.

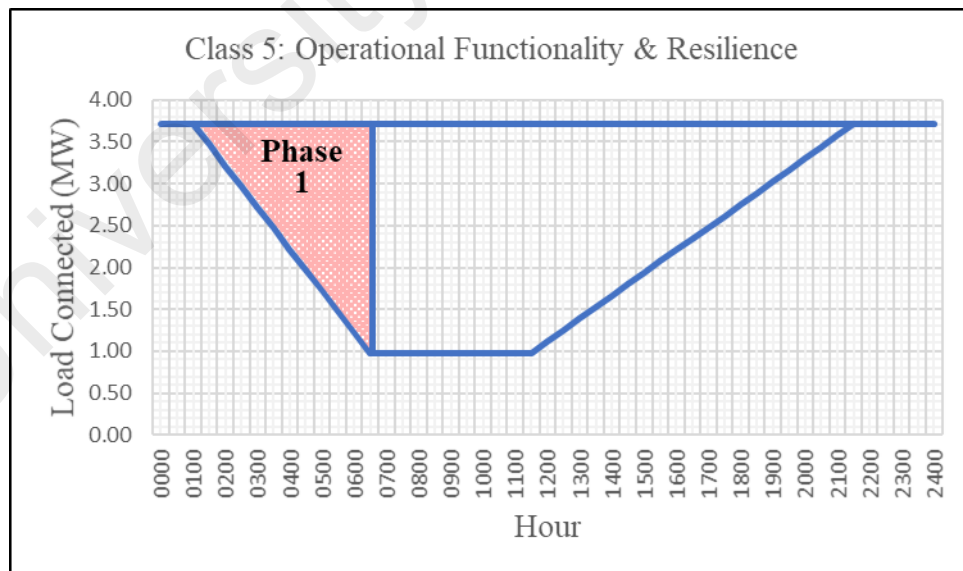


Figure 4.15: Most-left Triangle in Resilience Trapezoid.

ii. Phase 2: Center Rectangle in Resilience Trapezoid

With the rectangle as shown in Figure 4.16, the degraded phase is plotted to represent the system's post-event functionality and resilience levels. The rectangle's horizontal line indicates that the duration in which the system remains in the same state before restoration work can start. Simply put, this rectangle represents the resilience loss over a waiting time before restoration can take place.

In this study, this waiting time is assumed to be 5 hours, however, in real world scenarios, many unforeseeable factors may be introduced into the degraded phase, which could either extend or shorten this duration. With this rectangle, enhancement strategies can be designed to increase resources and efficiency of restoration efforts for the purpose of reducing the amount of waiting time.

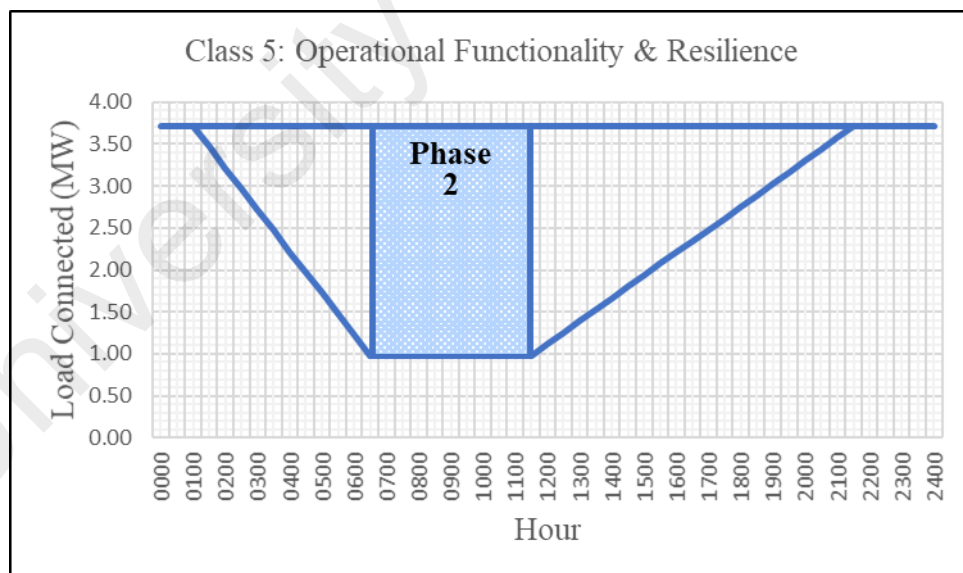


Figure 4.16: Center Rectangle in Resilience Trapezoid.

iii. Phase 3: Most-right Triangle in Resilience Trapezoid

With the triangle as shown in Figure 4.17, the recovery phase is plotted to represent the system's functionality and resilience which are gradually recovering. Similar to the resilience triangle assessment method, ideally, the gradient of the triangle's hypotenuse should be as steep as possible, to indicate a rapid recovery rate.

In this study, the triangle's hypotenuse is plotted as a linear line, however, in real world scenarios, many unforeseeable factors may be included into the restoration stage. In reality, the triangle's hypotenuse may be exponential or even triangular, subject to the actual environment and unpredictable factors. However, to reduce the complexity of the assessment, a linear line can be mapped to estimate the recovery rate of the system. With this triangle, enhancement strategies can be designed aimed at increasing resources and efficiency of restoration efforts to reduce the restoration time and thus increasing the recovery rate of the system.

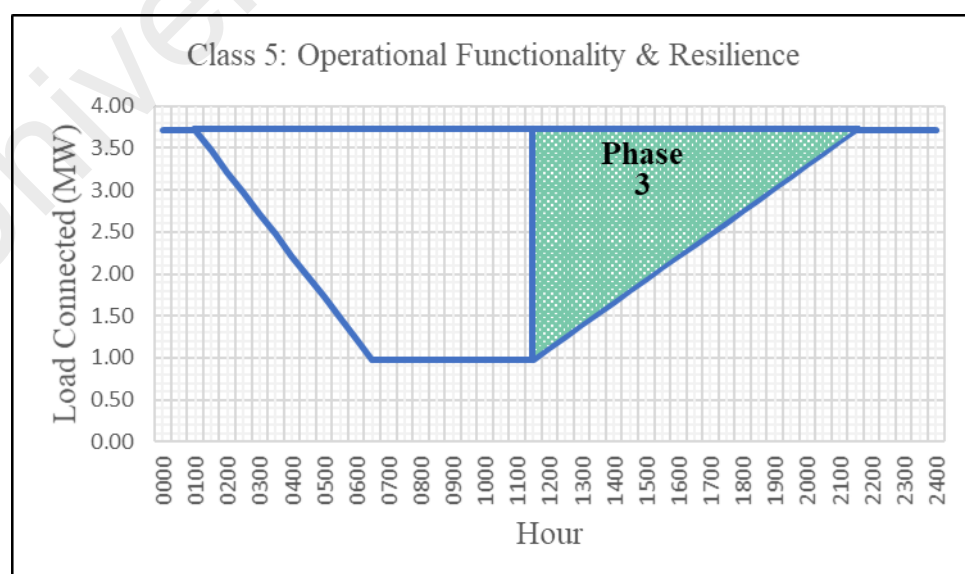


Figure 4.17: Most-right Triangle in Resilience Trapezoid.

4.6.3 Evaluation of the Code-Based Resilience Metrics Assessment Method

The adaptation of the code-based resilience metrics assessment method has demonstrated that this approach is generally useful for high level evaluation of a system's state of functionality and resilience. Although the code-based metric approach is able to quantify numerically, the resilience of a system with the use of a scale of specified range of resilience metrics, it does not address critical factors and phases in which the system succumbs to. While the code-based metric is straightforward in its approach, which presumably might require minimal training for its users, the same inference could be drawn when observing the resilience triangle and resilience trapezoid approaches.

Perhaps the most significant advantage of code-based metric, is the usage of its resilience metric scaling and variable categorization. In addition to quantifying the state of resilience of a system, it could also be useful in projecting and categorizing the intensity of an impact caused by a high-impact, low-probability event. As each event is logged and categorized, a library of historical data can be gathered to assist in decision-making for similar occurrences in the future, as shown in Table 4.18.

Table 4.18: Resilience variable categorization.

Resilience Variable	Duration of Event	Possible nature of disruption
A	<i>below 10^6 secs</i>	Event which disrupted other infrastructures and crew availability
B	<i>below 10^5 secs</i>	Widespread disruptions covering large areas and black-start generators
C	<i>below 10^4 secs</i>	Pole and equipment damages
D	<i>below 10^3 secs</i>	Line and equipment damages
E	<i>below 10^2 secs</i>	Blown fuse caused by overcurrent
F	<i>below 10^1 secs</i>	Line-to-line fault, voltage dips, recloser issues

4.6.4 Summary of Evaluation

From the earlier segments, the merits and disadvantages of each assessment method can be summarized as shown in Table 4.19.

Table 4.19: Summary of evaluation.

	Resilience Triangle	Resilience Trapezoid	Code-Based Metric
Advantages	Easy to use	Easy to use	Easy to use
	Can be used to assess operational and infrastructural resilience	Can be used to assess operational and infrastructural resilience	Can be used to assess operational and infrastructural resilience
	Indicates loss of functionality and resilience	Indicates loss of functionality and resilience	Indicates loss of functionality and resilience
	Indicates recovery phase	Indicates degradation, degraded, and recovery phase	Categorizes resiliency with specified scaling
	Provides visuals of data mapping in graphical form	Provides visuals of data mapping in graphical form	Categorized impact of event with specified variables
Disadvantages	Linear plotting of recovery rate	Linear plotting of recovery rate	No graphical mapping to indicate functionality and resilience levels
	Does not include degradation and degraded phase	Linear plotting of degradation	Does not include degradation and degraded phase
	Analyses one event at a time	Analyses one event at a time	Analyses one event at a time

CHAPTER 5: CONCLUSION

5.1 Closing Summary

By carrying out this study, a 33-bus distribution system's functionality and resilience were evaluated in 3 separate scenarios defined by 3 individual NESC pole classes by adapting 3 different resilience assessment methods. Subsequently, comparisons are made to reflect the different attributes of each resilience assessment method.

While each resilience assessment method has its own set of merits and disadvantages, the resilience trapezoid assessment method allows a more comprehensive evaluation of a system's functionality and resilience as it projects the system's state phase-by-phase. Since the resilience trapezoid can be dissected into three areas which represent three individual phases, evaluations can be carried out on each phase, in which mitigation and prevention strategies could also be specifically planned and ultimately adapted for each phase. However, the linear gradients of the resilience trapezoid in the degradation and recovery phases, may only provide a constant rate of change. As emphasized in earlier segments, in real world scenarios, the degradation and recovery undergone by a system could vary or even be exponential.

Lastly, since few of the necessary parameters such as post-event functionality levels and duration of event are common between the resilience trapezoid and code-based resilience metric assessment methods, a hybrid or combination of both methods could perhaps result in an assessment with more depth notably in the area of categorization of impact for each phase.

5.2 Future Works

The topic of “resilience” is relatively new in comparison with topics such as reliability, security, adequacy, and many others. Thus, there lies a vast potential for more research and studies to add to the current existing body of knowledge.

Subsequent works similar to that of which was carried out in this study, is recommended for the near future, as this would serve the interest of the continuity on this specific subject. Succeeding works should firstly focus on conducting more vigorous assessments with the hybrid framework proposed in the earlier segment, which consist of the resilience trapezoid and the code-based metric. This hybrid framework should also be evaluated against another form of resilience assessment method. Additionally, the proposed assessment should be carried out with different parameters as shown in the below.

- i. Different distribution systems

Different types of distribution systems of either larger or smaller networks, consisting of features such as tie-lines and distributed generation, should be assessed with the hybrid framework and alternative assessment methods.

- ii. Different high-impact, low-probability event

Different types of extreme weather scenario such as snowstorms, floods, solar storms, and many others, and the impact of each on distribution systems should be assessed with the hybrid framework and alternative assessment methods.

Lastly, to extend the works carried out in this study, emphasis should be placed on enhancement strategies for each phase undergone by a distribution system affected by a high-impact, low-probability event.

REFERENCES

- Abi-Samra, N. C., & Malcolm, W. P. (2011). Extreme Weather Effects on Power Systems. *2011 IEEE Power and Energy Society General Meeting*. Detroit, MI: IEEE.
- Ali, K., Wiyagi, R. O., & Syahputra, R. (June, 2017). Reliability Analysis of Power Distribution System. *Journal of Electrical Technology UMY*, 1(2), 67-74.
- Anwar, A., & Mahmood, A. N. (2014). Cyber Security of Smart Grid Infrastructure. *The State of the Art in Intrusion Prevention and Detection*, 449-472.
- Ayyub, B. M. (2014). Systems Resilience for Multihazard Environments: Definition, Metrics, and Valuation for Decision Making. *Risk Analysis*, 34(2), 340-355.
- Baran, M. E., & Wu, F. F. (April, 1989). Network Reconfiguration in Distribution Systems for Loss Reduction and Load Balancing. *IEEE Transactions on Power Delivery*, 4(2), 1401-1407.
- Bie, Z., Lin, Y., Li, G., & Li, F. (2017). Battling the Extreme: A Study on the Power System Resilience. *Proceedings of the IEEE*. 107, pp. 1253-1266. IEEE.
- Billington, R., Wu, C., & Singh, G. (2002). Extreme adverse weather modeling in transmission and distribution system realibility evaluation. *Proceedings of the Power Systems Computational Conference, Session 13*. Sevilla.
- Borges Hink, R. C., Beaver, J. M., & Buckner, M. A. (2014). Machine learning for power system disturbance and cyber-attack discrimination. *2014 7th International Symposium on Resilient Control Systems (ISRCs)*, (pp. 1-8). Denver, CO.
- Bouhouras, A. S., Marinopoulos, A. G., Labridis, D. P., & Dokopoulos, P. S. (2010). Installation of PV systems in Greece-Reliability improvement in the transmission and distribution system. *Electric Power Systems Research*, 547-555.
- Brown, R. (2009). *Cost-Benefit Analysis of the Deployment of Utility Infrastructure Upgrades and Storm Hardening Programs*. Quanta Technology.
- Brown, R. E. (2008). *Electric Power Distribution Reliability* (Second ed.). CRC Press.
- Cabinet Office. (2011). *Keeping the Country Running: Natural Hazards and Infrastructure*. United Kingdom.
- Calrson, L., Bassett, G., Buehring, W., Collins, M., Folga, S., Haffenden, B., . . . Whitfield, R. (2012). *Resilience: Theory and Applications*. Argonne, IL: Argonne National Lab (ANL).
- Campbell, R. J. (2012). *Weather Related Power Outages & Electric System Resiliency*. Washington, DC: Congressional Research Service.

- Chanda, S., Srivastava, A. K., Mohanpurkar, M. U., & Hovsopian, R. (August, 2018). Quantifying Power Distribution System Resiliency Using Code-Based Metric. *IEEE Transactions on Industry Applications*, 54(4), 3676-3686.
- Chang, G. W., Chu, S. Y., & Wang, H. L. (May, 2007). An Improved Backward-Forward Sweep Load Flow Algorithm for Radial Distribution Systems. *IEEE Transactions on Power Systems*, 22(2).
- Cimellaro, G. P., Reinhorn, A. M., & Bruneau, M. (2010). Seismic resilience of a hospital system. *Structure and Infrastructure Engineering*, 6(1-2), 127-144.
- Clark, D. (15 December, 2011). *How will climate change affect rainfall?* Retrieved from The Guardian: <https://www.theguardian.com/environment/2011/dec/15/climate-change-rainfall>
- Dunford, R., Su, Q., Tamang, E., & Wintour, A. (2014). The Pareto Principle. *The Plymouth Student Scientist*, 7(1), 140-148.
- Dunn, S., Wilkinson, S., Alderson, D., Fowler, H., & Galasso, C. (February, 2018). Fragility Curves for Assessing the Resilience of Electricity Networks Constructed from an Extensive Fault Database. *Natural Hazard Review*, 19(1).
- Esfahani, P. M., Vrakopoulou, M., Margellos, K., Lygeros, J., & Andersson, G. (2010). Cyber attack in a two-area power system: Impact identification using reachability. *Proceedings of the 2010 American Control Conference*, (pp. 962-967). Baltimore, MD.
- Eskandarpour, R., Khodaei, A., & Lin, J. (2016). Event-driven security-constrained unit commitment with component outage estimation based on machine learning method. *2016 North American Power Symposium (NAPS)*, (pp. 1-6). Denver, CO.
- Espinoza, S., Panteli, M., Mancarella, P., & Rudnick, H. (March, 2016). Multi-phase assessment and adaptation of power systems resilience to natural hazards. *Electric Power Systems Research*, 136, 352-361.
- Fogarty, D., & Tan, A. (25 September, 2019). *Rising oceans and melting ice caps pose dire threats unless emissions are cut: UN IPCC report.* Retrieved from The Strait Times: <https://www.straitstimes.com/world/rising-oceans-and-melting-ice-caps-pose-dire-threats-unless-emissions-are-cut-un-report>
- Holling, C. S. (1973). Resilience and stability of ecological systems. *Annual review of ecology and systematics*, 4(1), 1-23.
- Horton, R., Boteler, D., Overbye, T. J., Pirjola, R., & Dugan, R. C. (October, 2012). A Test Case for the Calculation of Geomagnetically Induced Currents. *IEEE Transactions on Power Delivery*, 27(4), 2368-2373.
- Hosseini, S., Baker, K., & Ramirez-Marquez, J. E. (January, 2016). A review of definitions and measures of system resilience. *Reliability Engineering & System Safety*, 145, 47-61.

- Kappenman, J. (January, 2010). Geomagnetic Storms and their Impacts on the U.S. Power Grid. (eBook). Goleta, CA: Metatech.
- Kappenman, J. G. (January, 2004). The Evolving Vulnerability of Electric Power Grids. *Space Weather*, 2(1).
- Kezunovic, M., Dobson, I., & Dong, Y. (2008). Impact of Extreme Weather on Power System Blackouts and Forced Outages: New Challenges.
- Kundur, P., Taylor, C., & Pourbeik, P. (2007). Blackout Experiences and Lessons, Best Practices for System Dynamic Performance, and the Role of New Technologies. *IEEE Task Force Report*.
- Li, Y., Xie, K., Wang, L., & Xiang, Y. (2019). Exploiting Network Topology Optimization and Demand Side Management to Improve Bulk Power System Resilience under Windstorms. *Electric Power Systems Research*, 171, 127-140.
- Lin, Y., & Bie, Z. (2016). Study on the Resilience of the Integrated Energy System. *Energy Procedia*, 103, 171-176.
- Lin, Y., Bie, Z., & Qiu, A. (Jan, 2018). A review of key strategies in realizing power system resilience. *Global Energy Interconnection*, 1(1), 70-78.
- Ma, S., Chen, B., & Wang, Z. (March, 2018). Resilience Enhancement Strategy for Distribution Systems Under Extreme Weather Events. *IEEE TRANSACTIONS ON SMART GRID*, 9(2), 1442-1451.
- Michiorri, A., & Taylor, P. C. (2009). Forecasting real-time ratings for electricity distribution networks using weather forecast data. *20th International Conference on Electricity Distribution*, (pp. 8-11). Prague.
- Michline Rupa, J. A., & Ganesh, S. (2014). Power Flow Analysis for Radial Distribution System Using Backward-Forward Sweep Method. *IJECECE*, 8(10), 1621-1625.
- Moloney, A. (September, 2017). *METRO UK*. Retrieved from What is the difference between a hurricane, a tornado and a tropical storm: <https://metro.co.uk/2017/09/07/what-is-the-difference-between-a-hurricane-a-tornado-and-a-tropical-storm-6909906/>
- National Electrical Safety Code*. (2007). IEEE.
- Orencio, P. M., & Fujii, M. (March, 2013). A localized disaster-resilience index to assess coastal communities based on an analytic hierarchy process (AHP). *International Journal of Disaster Risk Reduction*, 3, 62-75.
- Ouali, S., & Cherkaoui, A. (January, 2020). An Improved Backward-Forward Sweep Power Flow Method Based on a New Network Information Organization for Radial Distribution Systems. *Journal of Electrical and Computer Engineering*, 2020.

- Panteli, M., & Mancarella, P. (October, 2015). Influence of Extreme Weather and Climate Change on the Resilience of Power Systems: Impact and Possible Mitigation Strategies. *Electric Power Systems Research*, 127, 259-270.
- Panteli, M., & Mancarella, P. (February, 2015). Modeling and Evaluating the Resilience of Critical Electrical Power Infrastructure to Extreme Weather Events. *IEEE Systems Journal*.
- Panteli, M., & Mancarella, P. (June, 2015). The Grid: Stronger, Bigger, Smarter? *IEEE Power and Energy Magazine*, 13(3), 58-66.
- Panteli, M., Mancarella, P., Trakas, D. N., Kyriakides, E., & Hatziargyriou, N. D. (November, 2017). Metrics and Quantification of Operational and Infrastructure Resilience in Power Systems. *IEEE Transactions on Power Systems*, 32(6), 4732-4742.
- Panteli, M., Pickering, C., Wilkinson, S., Dawson, R., & Mancarella, P. (September, 2017). Power System Resilience to Extreme Weather: Fragility Modeling, Probabilistic Impact Assessment, and Adaptation Measures. *IEEE Transactions on Power Systems*, 32(5).
- Panteli, M., Trakas, D. N., Mancarella, P., & Hatziargyriou, N. D. (2017). Power Systems Resilience Assessment: Hardening and Smart Operational Enhancement Strategies. *Proceedings of the IEEE*. 105, pp. 1202-1213. IEEE.
- Pasqualetti, F., Dorfler, F., & Bullo, F. (2011). Cyber-Physical Attacks in Power Networks: Models, Fundamental Limitations and Monitor Design. *2011 50th IEEE Conference on Decision and Control and European Control Conference* (pp. 2195-2201). Orlando, FL: IEEE.
- Roegel, P. E., Collier, Z. A., Mancillas, J., McDonagh, J. A., & Linkov, I. (2014). Metrics for energy resilience. *Energy Policy*.
- Rosendo, J. A., Gomez-Exposito, A., Tevar, G., & Rodriguez, M. (April, 2008). Evaluation and Improvement of Supply Reliability Indices for Distribution Networks. *IEEE/PES Transmission and Distribution Conference and Exposition*, 1-6.
- Schott, T., Landsea, C., Hafele, G., Lorens, J., Taylor, A., Thurm, H., . . . Zaleski, W. (2010). *The Saffir-Simpson Hurricane Wind Scale*. Retrieved from NOAA/National Weather Service: <https://origin.www.nhc.noaa.gov/pdf/sshws.pdf>
- Schrijver, C. J., & Mitchell, S. D. (2013). Disturbances in the US electric grid associated with geomagnetic activity. *Journal of Space Weather and Space Climate*, 3.
- Sekhar, P. C., Deshpande, R. A., & Sankar, V. (2016). Evaluation and Improvement of Reliability Indices of Electrical Power Distribution System. *National Power Systems Conference (NPSC)*, 1-6.
- Shahid, S. (2012). Vulnerability of the power sector of Bangladesh to climate change and extreme weather events. *Regional Environmental Change*, 12, 595-606.

- Thomsom, A. W., McKay, A. J., Clarke, E., & Reay, S. J. (2005). Surface electric fields and geomagnetically induced currents in the Scottish power grid during the 30 October 2003 geomagnetic storm. *Space Weather*, 3(S11002).
- Tierney, K., & Bruneau, M. (2007). Conceptualizing and Measuring Resilience. *TR News*, 14-17.
- Veeramany, A., Unwin, S. D., Coles, G. A., Dagle, J. E., Millard, D. W., Yao, J., . . . Gourisetti, S. N. (2016). Framework for Modeling HighImpact, Low-Frequency Power Grid Events to Support RiskInformed Decisions. *International Journal of Disaster Risk Reduction*, 125-137.
- Watson, J.-P., Guttromson, R., Silva-Monroy, C., Jeffers, R., Jones, K., Ellison, J., . . . Walker, L. (2015). *Conceptual Framework for Developing Resilience Metrics for the Electricity, Oil, and Gas Sectors in the United States*. Sandia National Laboratories. Sandia National Laboratories.
- Zimmerman, R. D., & Murillo-Sanchez, C. E. (2019). MATPOWER. doi:10.5281/zenodo.3251119
- Zobel, W. C. (2010). Comparative Visualization of Predicted Disaster Resilience. *Proceedings of the 7th International ISCRAM Conference*. Seattle, USA.